Eutectic Electrolytes Chemistry for Rechargeable Zn Batteries

*Xuejun Lu [a], Evan J Hansen [a], Guanjie He [b, c], Jian Liu [a]**

[a] School of Engineering, Faculty of Applied Science, University of British Columbia, Kelowna, BC V1V 1V7, Canada

[b] Christopher Ingold Laboratory, Department of Chemistry, University College London, 20 Gordon Street, London, WC1H 0AJ UK

[c] Electrochemical Innovation Lab, Department Chemical Engineering, University College London, London, WC1E 7JE UK

** Corresponding author: Jian.liu@ubc.ca*

Abstract

Rechargeable zinc batteries (RZBs) have protruded to be promising candidates alternately compelling Lithium-ion batteries due to their low cost, inherent safety, and environmentally benign features. While designing cost-effective electrolyte systems with excellent compatibility with electrode materials, high energy/power density as well as long life-span challenge their further application as grid-scale energy storage devices. Eutectic electrolytes as a novel class of electrolytes have been extensively reported and explored taking advantage of their feasible preparation and high tunability. Recently, some perspectives have summarized the development and application of eutectic electrolytes in metal-based batteries, but their infancy elucidates further attention and discussion. This review systematically presents the fundamentals and definitions of eutectic electrolytes. Besides, a specific classification of eutectic electrolytes and their recent progress and performance on RZB fields are introduced as well. Significantly, we dissert the impacts of various composing eutectic systems for critical RZB chemistries including attractive features at electrolyte/electrode interfaces and ions/charges transport kinetics. The remaining challenges and proposed perspectives are ultimately induced, which deliver opportunities and offer practical guidance for the novel design of advanced eutectic electrolytes for superior RZB scenarios.

Keywords: deep eutectic solvents, hydrogen bonds, eutectic electrolytes, hydrogen bonding complex, rechargeable Zn batteries

1. Introduction

Rechargeable batteries (RBs) have been considered one of the advanced energy storage systems for storing renewable energy, which extensively accelerates sustainable economic and social development in electrical energy storage (EES).[1] Since the first commercialization by Sony Corporation in the 1990s, lithium-ion batteries (LIBs) have successfully dominated the EES market, including electronic communication devices and electric vehicles.[2] However, the limited lithium resources, fluctuant price, and safety issues of current LIBs have driven the research for alternative energy storage solutions in multiple application scenarios. As alternatives, battery chemistries based on the employment of multivalent charge carriers (*e.g.*, Zn^{2+}, Mg^{2+}, Ca^{2+}, and Al^{3+}) have received extensive attention.[2-3] Compared to LIBs and other energy storage systems, rechargeable zinc batteries (RZBs) exhibit great potential for large-scale energy storage applications, owing to the following features: (1) high theoretical capacity (~ 820 mAh g^{-1}) and low electrochemical potential (−0.763 V *versus* the standard hydrogen electrode (SHE)) of Zn metal (**Figure 1**a);[4] (2) high ionic conductivity in aqueous electrolytes due to compatible cation and hydrated radius of Zn^{2+} (**Figure 1**b);[5] (3) high energy density of Zn anode resulting from two-electron transfer during redox reactions; (4) excellent ambient stability, low cost, and nontoxicity of Zn; (5) facile material processing and battery manufacturing.[6] Therefore, RZBs have attracted tremendous research interest in last two decades. Among RZBs, Zn-ion batteries (ZIBs) and Zn-air batteries (ZABs) have occupied nearly half research fields of RZBs since 2006 (**Figure 1**c), where a variety of RZBs configurations regarding cathode designs (*i.e.*, Ni-based (NiO, $Ni(OH)_2$), Co-based CoO, Co_3O_4), and Mn-based (α-MnO_2, γ-MnO_2) cathodes, *etc.*) were applied.[7] In addition, emerging high-performance RZBs that further accelerate application scenarios of needs, including Zn redox-flow batteries (ZRFBs) with long cycling stability,[8] and Zn solid-state batteries (ZSSBs) with an ultrahigh specific capacity.[9] Particularly, Chao et al. reviewed the roadmap for advanced aqueous Zn batteries (AZBs) from material designs to applications, which showed the state of the art on

AZBs depending on various prototypes and recommended commercialization of next-generation reliable AZBs.[5]

To date, many efforts have been invested in profound studies for the combination of electrodes and configurations of RZBs, of which some have dominated the current primary battery market.[10] Cao et al. recently summarized numerous strategies including host materials optimization, artificial functional layers construction, and electrolyte composition modulation to regulate Zn^{2+} solvation structures with the suppression of the dendrite and side reaction in ZIBs.[11] However, there are still many challenges remaining in the routine use of liquid electrolytes: (1) Zn anode-related issues, including uneven electrodeposition, limited reversibility, hydrogen evolution, and Zn dendrite formation and passivation; (2) cathode-related issues, including cathode dissolution, byproducts phase change, and structure collapse; (3) limited voltage windows of liquid electrolytes, resulting from physico-/electro-chemical stability and solubility limitation of active substances; (4) high charge density of Zn^{2+}, causing sluggish Zn-ion diffusion associated with the development and utilization of high-performance cathode materials. Apart from these designs of new chemistry and structures for high-capacity and stable electrode materials, another significant role of the electrolyte enables the successful function of electrode materials and chemistries. On the one hand, Zn anodes, commonly used with alkaline electrolytes, suffer from vulnerable corrosion, surface passivation, and dendritic growth.[12] On the other hand, water consumption and low Coulombic efficiency (*CE*) caused by side reactions of Zn still limit the research evolution of acidic or neutral electrolytes for RZBs.[13] Thus, emerging high-performance electrolytes has driven the explorations from multi-paths for enhanced RZBs properties, including electrochemical stability, operational potential window, deposition/dissolution efficiency of the Zn anode, and electrochemical reaction mechanism.[6b, 7a]

Among electrolyte designs, the engineering operated from species and combination of solvents and metal salts, synthesis and employment of ionic liquids (ILs) and deep-eutectic-solvents (DESs), and regulation of solvation and coordination structure promotes the realistic application of RZB configurations.[14] For instance, so-

called “solvent-in-salt” (SIS) electrolytes have been proposed by Suo *et al.*,[15] demonstrated the presence of unusual properties to distinguish SIS electrolytes from traditional ones if either the weight or volume ratio of salt to solvent exceeds the number of 1.0. Then followed in 2015, Suo *et al.* invented 21 molality (m) “water-in-salt” (WIS) electrolytes dedicating a compromise among extended electrochemical stability window (ESW), cost, and safety for LIBs.[16] Similarly, these highly concentrated electrolytes or WIS electrolytes have been applied frequently in ZIBs to determine the participation of solvent molecules surrounding Zn cation solvation shells.[17] Interestingly, the use of “water-in-bi-salt” (WIBS) and “co-solvent-in-salt” (CSIS) electrolytes further helped reduce Zn dendrites, prevent capacity fading and maintain high *CE*.[13, 18] Meanwhile, some practical outcomes point out uncertainties regarding WIS or super-concentrated electrolyte systems containing water, such as poor temperature stability at the diverse environment, the drying-out phenomenon occurred with continuous electrolyte consumption during charge-discharge and cycling process, and unstable solid-electrolyte-interphase (SEI) formation of anodes.[19]

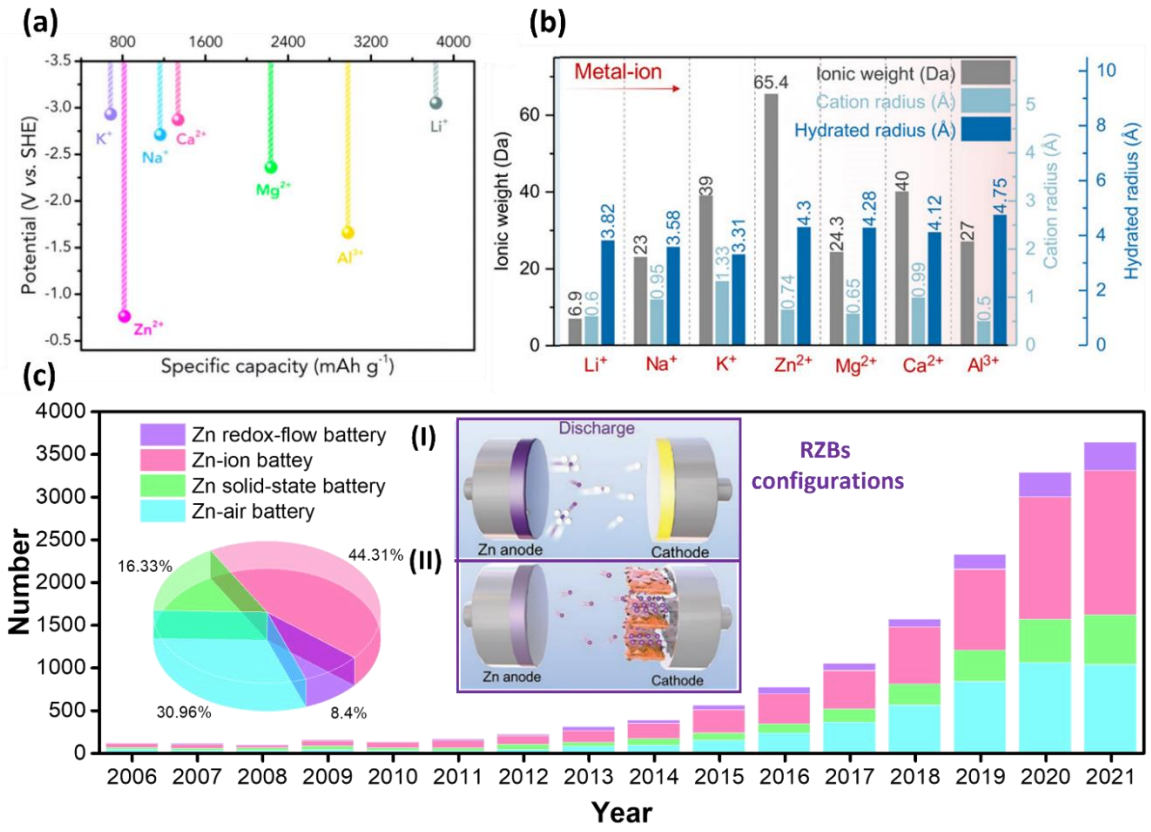

Figure 1. (a) Comparison of standard electrode potentials and theoretical capacities of various metal anodes. Reproduced with permission.[7a] Copyright 2021, American Chemical Society. (b) Comparison of cation radius and hydrated radius of the typical metal-ion charge carriers. Reproduced with permission.[5] Copyright 2020, American Association for the Advancement of Science. (c) The number of publications devoted to different RZBs according to Web of Science (until Nov. 30th, 2021). Inserted schematics of the basic structure for RZBs, (I) Zn anode//Ni-/Co-/Air-based cathode; (II) Zn anode//Mn-/V-/PBA-/Organic-based cathode. Reproduced with permission.[7b] Copyright 2020, WILEY-VCH.

These days, ILs, the class of liquid solvents, act as promising candidates for batteries and are composed primarily of one type of discrete anion and cation with a melting point below 100 °C.[20] ILs for EESs are desirable due to their low vapor pressure, wide ESW, and high physical, chemical, and thermal stability. Specifically, benefits for RZBs raised from ILs have been elucidated, such as inhibiting the corrosion of the zinc anode and the hydrogen evolution during cycling, widening the ESW, and restraining Zn dendrite growth while exhibiting relatively flat voltage profiles.[9b, 21] Although coulombic interactions and van der Waals interactions between ILs' cations and anions have a substantial influence on these characteristics, applying IL-based electrolytes in industrial batteries met encumbrances, initially due to their uplifted viscosity and related poor diffusion of charges, further the insufficient formation of an IL-derived SEI.[22] DESs resemble ILs (or IL analogues), widely acknowledged because of shared characteristics and properties (*i.e.*, simple synthesis, low cost, and good biocompatibility).[23] Recently, "designer electrolytes" honored DESs due to their high designability and moldability compared with conventional solvents and electrolytes, allowing energy storage and conversion technology of supercapacitors (SCs) and batteries.[24] For instance, an "aqueous-eutectic-in-salt" (AEIS) electrolyte has been reported by inducing the eutectic mixture of dimethyl sulfoxide (DMSO) and H_2O (with a molar ratio of 1:2). This eutectic electrolyte formed with the addition of Li bis(trifluoromethanesulfonyl)imide (LiTFSI) salts at near-saturation conditions resulted in excellent SC performance, especially when operating over a wide range of

extreme ambient temperatures (from –35 to +65 °C).[25] Recently, acetonitrile (CH_3CN) co-solvent added in AEIS helps form a new "tri-solvent-in-salt" system, which offers formation of an electrochemically active hydrogen bond (H-bond) complex as enhanced eutectic electrolytes.[26] It was also found that Li-based DESs served as remarkable candidates to replace IL or Li salt mixtures in LIBs because of their single-cation species, supporting a relatively high Li^+ transference number.[27] Xu et al. reported a 4.5 m LiTFSI–KOH–$CO(NH_2)_2$–H_2O non-flammable ternary eutectic electrolyte, which expands the ESW (>3.3 V) by forming a robust solid–electrolyte interphase. The resulting $Li_{1.5}Mn_2O_4$ || $Li_4Ti_5O_{12}$ pouch cells setting with this ternary eutectic electrolyte demonstrate a promising approach towards safe and low-cost aqueous LIBs.[28] Wang et al. proposed an economical room-temperature inorganic hydrated molten salt (RTMS) electrolyte, composed of low-cost lithium nitrate hydrate and sodium nitrate with a large ESW of 3.1 V. Based on this RTMS electrolyte, a hybrid Li/Na-ion full battery is fabricated exhibiting a high capacity of 139 mAh g^{-1} at 1 C and the capacity retention of 94.7% over 500 cycles at 3 C.[29] Meanwhile, DESs recently have been widely studied as electrolytes for Zn-based batteries because of their good stability in the air and moisture and strong water-miscibility, which are compatible with Zn metal considering the intensity of oxygen and humidity. Beyond DES-based electrolytes, "solvate ionic liquid" and other type ones presenting different interaction mechanisms (as introduced in **Figure 3**) contribute to the eutectic-electrolytes family.[14b, 30]

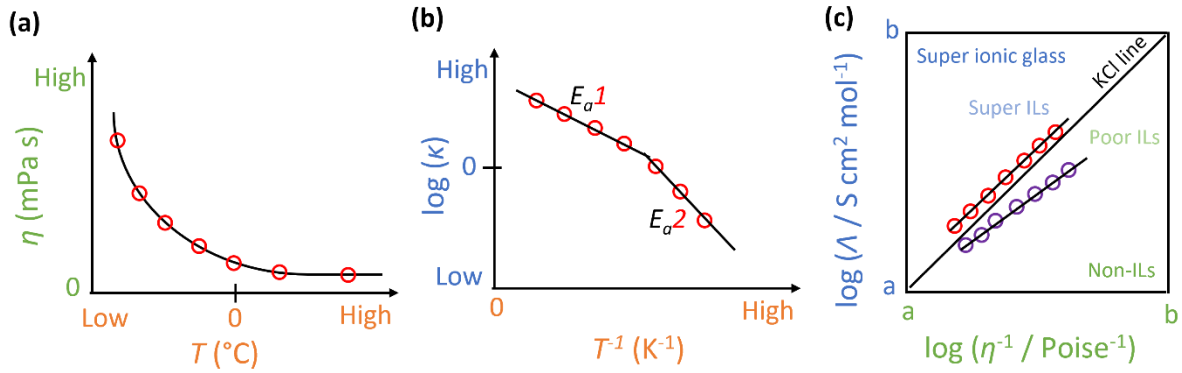

Figure 2. Schematic plots of various representative correlations for eutectic electrolytes. (a) The plot of viscosity *vs.* temperatures. (b) Arrhenius plot, inserting activation

energies (E_a1, E_a2) obtained from linear regression. (c) Walden plot, presenting aqueous KCl solutions as the "ideal" Walden line.

So far, several reports have comprehensively reviewed the fundamental physicochemical properties of eutectic electrolytes, taking the critical parameters related to EES applications: (1) negative correlation of viscosity (η) versus temperature (T, °C), which affects mass transport within the eutectic electrolytes along with T (**Figure 2**a);[24, 31] (2) positive correlation of ionic conductivity (κ) versus T (K), where κ of an eutectic electrolyte is much higher than conventional ILs because of the decreased the cation size and increased free volume, following an Arrhenius manner with large values for the activation energy (E_a) (**Figure 2**b);[23, 32] (3) linear correlation of molar conductivity (Λ) versus η, attributed to the validity of the Walden rule and proved hole theory that the holes limit charge transport instead of ions at infinite dilutions (**Figure 2**c).[33] Apart from these, features of low vapor pressure and high thermal decomposition temperature, make eutectic mixtures ideally nonflammable electrolytes comparing to the instability and volatility of organic electrolytes. Besides, other safety-related parameters involving chemical/electrochemical/thermal stability, allow eutectic electrolyte systems to show their positive potential impact on energy storage devices for making safe electrolytes.[24, 31-32, 34] In actuality, some efforts have been devoted to employing eutectic electrolytes on Zn-based batteries, following fruits illustrated the merits of using eutectic characteristics. While few reports concluded specific explanations about the physicochemical properties and formation mechanisms of eutectic electrolytes, they mainly focused on the applications of individual composition fixing mere issues raised from Zn anode or SEI.[10a, 14b, 35]

In this review, we introduce the definition of eutectic electrolytes distinguished from ILs, and diverse categories regarding combinations among salt, solvent, additive, and molar ratios. We also illustrate interaction mechanisms within eutectic electrolytes when occurring the formation/interruption process of H-bonds, and regulation of ions/molecules coordination structure or Zn^{2+} solvation structure through eutectic effects. Importantly, highlighted applications of eutectic electrolytes for various directions of RZBs are presented detailly. Hopefully, essential perspectives provided in

this discussion pave a path for the future exploration of eutectic electrolyte systems in energy storage fields.

2. Definition of eutectic electrolytes

DESs were firstly studied by Abbott *et al.* in 2001, using a range of quaternary ammonium salts heated with $ZnCl_2$ to realize resulting liquids with low melting points (23−25 °C).[20] Followed by 2003, Abbott *et al.* proposed the formation of liquid eutectic electrolyte, preliminary generated through H-bond interactions between choline chloride (ChCl) and urea (**Figure 3**a). The formed H-bonds increased the eutectic's effective size, which, in turn, reduced the chloride anion interaction with the ammonium cation of ChCl, introducing melting points much lower than those of their pure compounds.[36] To extend this initial study, DESs have been described as eutectic mixtures of Lewis or Brønsted acids and bases, which can contain a variety of anionic and/or cationic species.[24] Typically, the obtained complexation of a quaternary ammonium salt with a metal salt or hydrogen bond donor (HBD) is presenting in DESs, where occurs the charge delocalization *via* H-bonds for the decreased melting point of the mixture compared to the individual component's ones. Feasible preparation of DESs determined by personal preference, equipment availability, and water-proof capacity requires no additional solvent, purification, and reaction, contributing economically novel liquids accessible as solvents and/or electrolytes for existing and forthcoming chemistries.[32, 34]

Depending on the feature of the utilized complexing agents, DESs are traditionally classified into five types, *i.e.*, Type I combines a quaternary ammonium salt and a metal chloride; Type II consists of a quaternary ammonium salt and a metal chloride hydrate; Type III forms from a quaternary ammonium salt and an HBD;[37] Type IV composes a metal chloride hydrate and HBD;[38] and Type V declares a relatively new class that consists of merely nonionic molecular HBDs and hydrogen bond acceptors (HBAs).[39] Whereas, these classify can be simplified in a general formula of Cat^+X^-zY as summarized by Smith *et al.* (**Figure 3**b),[32] where Cat^+ is principally representing ammonium, phosphonium, or sulfonium cation, X^- represents a Lewis base (*i.e.*, a

halide anion), Y denotes a Lewis or Brønsted acid, and z refers to the interacted number of Y molecules. Besides, the solid-liquid equilibria phase diagram represents the relational phase behavior of a binary mixture composed of pure compounds A and B, where T_E reveals the lowest melting point for the "deep" eutectic solvent.[23] Thus ΔT_1 is the magnitude attributed to the interaction between A and B, which is larger along with increased interaction.

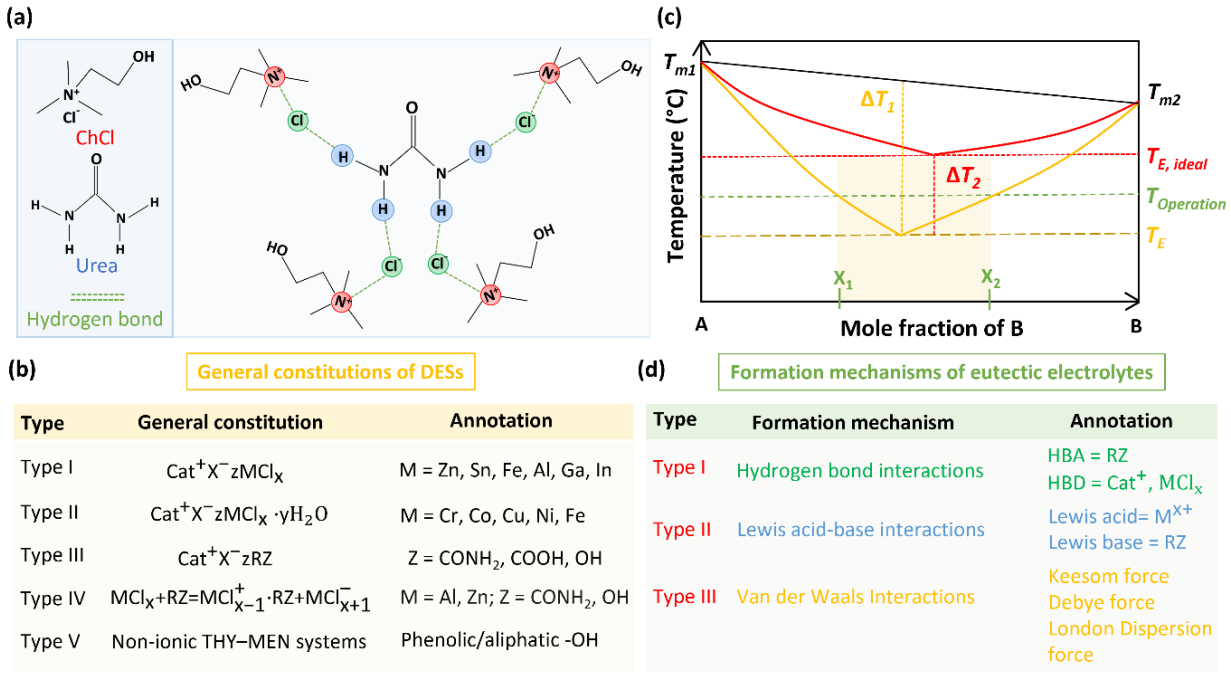

(b) General constitutions of DESs

Type	General constitution	Annotation
Type I	$Cat^+X^-zMCl_x$	M = Zn, Sn, Fe, Al, Ga, In
Type II	$Cat^+X^-zMCl_x \cdot yH_2O$	M = Cr, Co, Cu, Ni, Fe
Type III	Cat^+X^-zRZ	Z = $CONH_2$, COOH, OH
Type IV	$MCl_x+RZ=MCl^+_{x-1}\cdot RZ+MCl^-_{x+1}$	M = Al, Zn; Z = $CONH_2$, OH
Type V	Non-ionic THY–MEN systems	Phenolic/aliphatic -OH

(d) Formation mechanisms of eutectic electrolytes

Type	Formation mechanism	Annotation
Type I	Hydrogen bond interactions	HBA = RZ HBD = Cat^+, MCl_x
Type II	Lewis acid-base interactions	Lewis acid= M^{x+} Lewis base = RZ
Type III	Van der Waals Interactions	Keesom force Debye force London Dispersion force

Figure 3. (a) Schematic representation of H-bond interactions between ChCl and urea. (b) Summary table of general constitutions for DESs. Reproduced with permission.[32] Copyright 2014, American Chemical Society. (c) Schematic evolution of the phase diagram for eutectic electrolytes. Reproduced with permission.[24] Copyright 2021, WILEY-VCH. (d) Summary table of formation mechanisms for eutectic electrolytes. Reproduced with permission.[40] Copyright 2020, American Chemical Society.

Recently, an updated definition for DESs has been ascribed as a mixture of two or more components, whereas the temperature at the eutectic point is below that of an ideal liquid mixture ($T_{E,\ ideal}$), as for the new temperature depression difference (ΔT_2) is defined between T_E and $T_{E,\ ideal}$. Interestingly, eutectic electrolytes act as a class of novel liquid mixtures composed in a certain range between the mole fraction range of X_1 and X_2 regarding ΔT_2 (**Figure 3**c).[24, 41] Furthermore, Zhang *et al.* recently concluded the

formation of eutectic electrolytes through the function of intermolecular interactions, which can be readily determined by comparing stronger interaction intensity of distinct components in resulting liquids than original each component.[40] Accordingly, three type interactions consists of formation mechanisms for identified eutectic electrolytes (**Figure 3**d), *i.e.*, H-bond interactions are regarded as the typical effect of formed DES-based eutectic electrolytes, relatively strong hydrogen bonding leads to the low-melting-point feature of electrolytes;[38, 42] Lewis acid−base interactions require a substance (referred to Lewis acid) accepting an electron pair donated from another one (referred to Lewis base). However, these interactions weakly affect the Lewis chemistry compared to covalent bond forces, instead of by altering the coordination state that results in decreased melting point of eutectic electrolytes;[1b, 40] Ultimately, van der Waals interactions are relatively weak among all chemical forces, while existing in eutectic mixtures are stronger than the primary molecular interactions of each component, but only a few reports related on van der Waals forces in eutectic electrolytes.[43]

Nevertheless, the physicochemical properties (*e.g.*, melting point, viscosity, ionic conductivity, surface tension, etc.) of eutectic electrolytes can be modified by taking advantage of different intermolecular interactions,[34] especially when selecting substituents, HBA/HBD species, ions size, composition ratios, and so on. For example, the melting point of acetamide-$Zn(TFSI)_2$ eutectic electrolytes shifts from −38 °C to −52 °C when molar ratio alters from 1:5 to 1:7;[44] notably, eutectic electrolytes composed of LiTFSI with urea and acetamide (in the same molar ratio of 1:5) show differed ionic conductivity of 0.21 and 1.6 mS cm^{-1} (at 25 °C), respectively, due to strong HBs through two NH_2 functionalities of urea, demonstrating the significance of strength regarding Lewis acid−base interactions formed from various Lewis bases.[45] Considering interaction impacts on the formation of eutectic electrolytes, we hence believe it's essential to propose advanced design strategies for optimizing the properties of eutectic electrolytes (see **Section 2.1**), especially when employing these electrolytes in RZB scenarios. Otherwise, well-characterized techniques help to understand the unique behavior of eutectic electrolytes. Therefore, regarding developing a

fundamental understanding, we will highlight experimental techniques and computing methods frequently adopted in the eutectic-electrolyte fields (see **Section 2.2**).

2.1. Design strategies

As illustrated above, eutectic electrolytes show many attractive properties for energy storage applications. **Figure 4**a compares merits of novel eutectic electrolytes with common mentioned electrolytes systems, including diluted/concentrated aqueous electrolytes, non-aqueous electrolytes, ionic liquids-based electrolytes, and DES-based electrolytes (*i.e.*, particularly, here we focus on the conventional compositions of DESs used for electrolytes according to Smith et al.[32]).[24, 46] Then, including wide potential window, excellent thermal/electrochemical stability as well as environmental benign because of non-toxicity, eutectic electrolytes display characteristics that are absent in the other electrolytes due to complexed anions and cations, such as non-flammability, high ionic conductivity, wide temperature window, high cost-saving efficiency, and feasible processability.[47] Meanwhile, eutectic electrolytes require non-additional solvent and/or reaction occurring during the synthesis process, introducing high utilization rate of substances and potential large-scale manufacture for eutectic electrolytes.[43b]

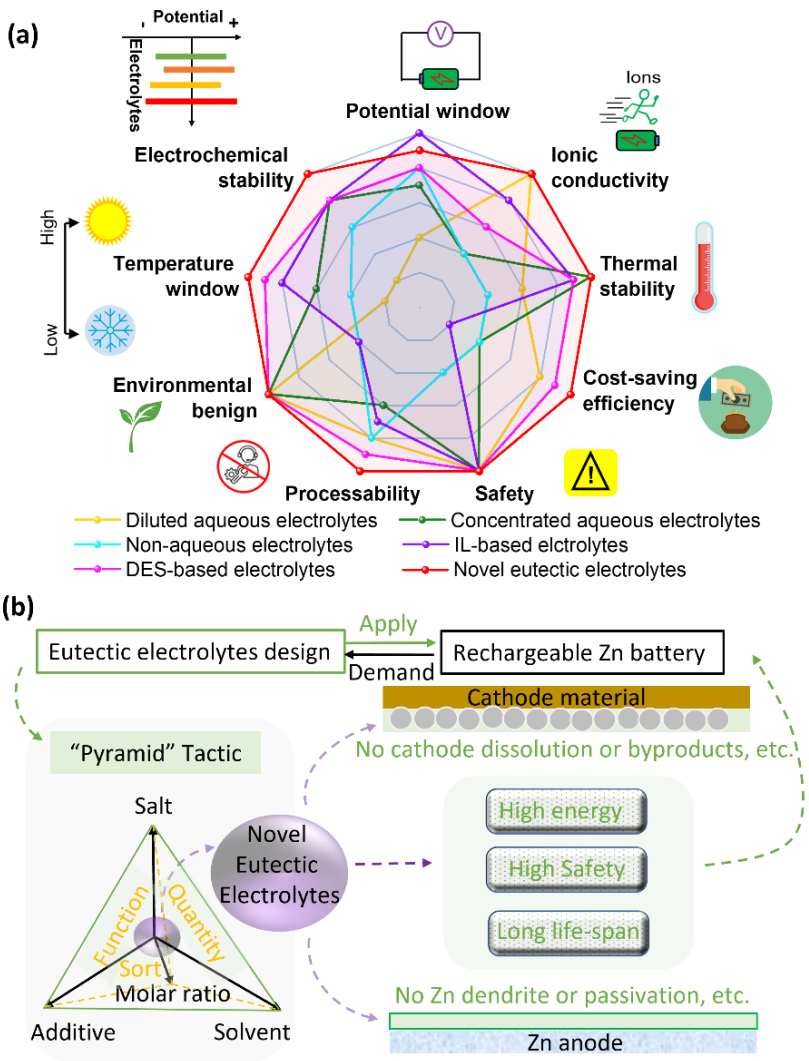

Figure 4. (a) Multi-angle comparison of eutectic electrolytes and other commonly used electrolyte systems. The diluted aqueous electrolytes keep low-cost and good ionic conductivity, but suffer from narrow electrochemical/temperature window and poor electrochemical stability; In contrast, concentrated aqueous electrolytes have various beneficial functions except for their major drawbacks of low ionic conductivity and high cost; Non-aqueous electrolytes usually cause environmental damage and show unstable thermal characteristic; Similarly, IL-based electrolytes are not economic and environmentally friendly, DES-based electrolytes need to further improve ionic conductivity and potential window.[24, 43b, 48] (b) Novel eutectic electrolytes design based on the "Pyramid" tactic demonstrates a highly flexible space with multi-dimensional features, and the influence of their physicochemical properties on both cathode material and Zn anode.[48c, 49]

To achieve optimal eutectic electrolytes, well-considered aspects related to each component's sorts, functions, and quantities based on specific formation mechanisms provide multidimensional approaches in designing desired eutectic systems for RZBs. Besides, it is also noted that electrolyte formulation of salt, solvent, additive, and molar ratio presents a profound influence on the Zn^{2+} solvation structure, interfacial stability, cathode dissolution, safety, and overall electrochemical performance of Zn-based batteries. Consequently, we propose a "Pyramid" tactic aiming at multi-angle thinking and implementing a new eutectic system modeling, combining eutectic electrolyte formulations and formation mechanisms to provide fundamental understanding and strategies (**Figure 4**b). According to this "Pyramid" tactic, it is plain to explore the old and new fashion of eutectic electrolytes, and further broaden applications and research of RZBs. For better comparison, some examples regarding reported electrolytes formulation composed from eutectics, effective functions for the improved electrochemical performance of RZBs, and advanced investigations for intrinsic mechanism will be depicted in **Section 3**.

2.2. Detection techniques

H-bonds work as the fundamentals for eutectic electrolytes, which are also the key intermolecular interaction during the formation of eutectic mixtures behind the depression of the melting point. However, it happens together with ionic contributions (from the anion/cation pair) and steric effects, which is hard to understand well by the actual behavior presented in the form of eutectic systems. As reported by IUPAC Recommendations,[50] H-bonds are inherently electrostatic delivering charge-transfer between HBDs and HBAs. Thus they are detectable through Raman spectroscopy, Fourier transform infrared spectroscopy (FTIR), Neutron scattering, and Nuclear magnetic resonance spectroscopy (NMR), *etc*. As a result, some experimental techniques are required to characterize and understand eutectic electrolytes appreciating the ongoing efforts on fundamental studies. This section will highlight major experimental techniques that are being employed and will be helpful for further exploitation.

Raman spectroscopy is used to verify the composition and purity of substances regarding eutectic electrolytes through observing molecular rotations, vibrations, and other low-frequency modes in a system. The observation depending on differences occurs between elastic and inelastic scattering when passing monochromatic wavelengths of light, which allows the identification of various molecules.[18b, 25, 51] Another helpful tool is ***FTIR*** used to confirm the structures of different molecules by obtaining a sample's infrared spectrum of emissions over a wide range of wavelengths.[52] FTIR is a valuable tool to get accurate information about the structure and identify impurities of eutectic electrolytes.[53] Verifying results between the two techniques will support the confirmed replicate parameters, widen the overall range of objects, and provide finer resolutions.

NMR is predominantly used to determine the presence and/or contributions of various functional groups in a liquid sample, ranging from verifying purity to identifying new functional groups using small shifts in resonance frequency for a given nuclear spin type.[36, 54] Regarding the analysis of eutectics' composition and structure, NMR experiments allow the quantification of electrolyte systems, following the conclusions based on the quantity of information, including impurities, water content, and slight shifts in functional group NMR signals (displaying the process of rearrangement and interaction within a structure).

Neutron scattering, provides insight into the structure and dynamics of materials over length scales (10^{-10} to 10^{-7} m) and time scales (10^{-11} to 10^{-6} s).[55] This technique uses contrast variation to supply the mechanism by highlighting portions of the inspective material, thus decisively taking advantage of this unique method to determine the complex structure and dynamics of eutectic mixtures. Otherwise, static and dynamic neutron scattering shows insight into the structure and dynamics of the H-bonding networks and ionic clusters treating a series of eutectics, exemplifying the neutron scattering that plays the significance in identifying eutectic chemistry.[56]

X-ray Scattering, also distinguished by small- and wide-angle X-ray scattering (SAXS and WAXS), are both essentially using X-rays to determine the structure of materials and verified through the analysis of maximum diffraction angles.[57]

Generally, SAXS is useful for detecting materials in longer-range ordering, but instead, WAXS is more sensitive to crystalline materials in short-range ordering. Thus, these techniques are frequently utilized to confirm the presence of micelle aggregates or microemulsions in eutectics and/or eutectic electrolytes.[58] Interestingly, eutectic electrolytes consist of concentrated salts sometimes equally treated as eutectic-in-salt (EIS) solutions because of the unique high-concentration feature, capturing the whole structure of formed clusters and aggregates of anion networks.[25-26, 59]

Dielectric relaxation spectroscopy (DRS), is a versatile tool for investigating the dipolar and ionic dynamics through polarization response of the material at the applied oscillating electric field.[60] DRS allows the correlations between microscopic mechanisms and macroscopic physical properties, including particular eutectic characteristics of ionic conductivity, viscosity, eutectic composition, *etc*. For instance, WIS-based eutectic electrolytes have been investigated by DRS with femtosecond IR spectroscopy demonstrating water dynamics (*i.e.*, the vibrational and rotational lifetimes), suggesting the solvation structures and local H-bonding networks in eutectic systems.[61]

Differential scanning calorimetry (DSC) and ***Thermogravimetric analysis (TGA)***, are jointly adopted thermo-analysis techniques. The one measures the heat amount that causes temperature change and helpfully examines latent heat during transformation events, gently occurring phase changes or, to a certain extent, glass transitions. As a result, DSC usually acts as the key for identifying melting points, formation enthalpies, heat capacity, and thermal stability of eutectic mixtures.[62] TGA is the other one that measures physical mass changes versus temperature and/or time, hypothesizing physical and chemical properties. Meanwhile, it is also helpful to investigate marked deviations and changes for phase changes due to the correlation between thermal behavior and physical properties. Regarding various thermal events (*e.g.*, absorption/ desorption, oxidation/reduction, sublimation, vaporization, and decomposition), it is evident that utilities DSC and TGA together as screening tools for potential behavior prediction of eutectic electrolytes.[25, 63]

3. Eutectic electrolytes for diverse RZB applications

The following section will summarize and discuss the recent applications of diverse eutectic electrolytes for RZBs, including a detailed classification of non-aqueous, aqueous, and solid eutectic systems (**Table 1**). Specifically, eutectic electrolyte optimization related to the electrolyte/electrode interphase and ions/charge transport will be presented as well.

Table 1. Summary for electrochemical performances of representative eutectic electrolytes in RZBs

Electrolytes	Cathode material	κ[a)] (mS cm^{-1})	ESW[a)] (V)	Specific capacity (mA h g^{-1})[a)]	Capacity retention[a)]	Ref.
Non-aqueous eutectic electrolytes						
5 M $ZnCl_2$-aceramide	Carbon	~1.00	1.30	90 **A h L^{-1}** (--)	--	Wang *et al.*[42]
ChCl-urea (Molar ratio 1:2)	δ-MnO_2	--	2.54	170 (50 mA g^{-1})	~50 % (0.1 A g^{-1}, 150 cycles)	Kao-ian *et al.*[64]
$Zn(TFSI)_2$-acetamide (Molar ratio 1:7)	V_2O_5	0.31	2.40	186 (100 mA g^{-1})	92.8% (0.6 A g^{-1}, 800 cycles)	Qiu *et al.*[44]
0.5 M $ZnCl_2$ + 0.5 M LiCl in 5 vol % AN/ChCl-urea (Molar ratio 1:2)	Sulfur	4.66	4.65	846 (0.5 A g^{-1})	~27.8% (2 A g^{-1}, 500 cycles)	Cui *et al.*[65]
1 M $CeCl_3$ in ChCl-EG (Molar ratio 1:2)	Graphite	1.32[b)]	2.20	0.1 **mA h** (0.5 mA cm^{-2})	~79% (0.5 mA cm^{-2}, 50 cycles)	Cao *et al.*[53]
Aqueous eutectic electrolytes						
urea/LiTFSI/$Zn(TFSI)_2$-30 mol.% H_2O	LMO/$LiFePO_4$	1.85	>2.50	117 (0.06 C)	86.6% (2 C, 600 cycles)	Zhao *et al.*[66]

7.5m $ZnCl_2$-H_2O	Polyaniline	73.30	--	~150 (1 A g^{-1})	~100% (0.2 A g^{-1}, 2000 cycles)	Zhang *et al.*[67]
1.3 m $ZnCl_2$-H_2O/DMSO	MnO_2	--	>2.20	~150 (8 C)	95.3% (8 C, 500 cycles)	Cao *et al.*[68]
2 M $Zn(CF_3SO_3)_2$-H_2O	V_2O_5	~60.00	>1.50	~430 (1 A g^{-1})	~95% (1 A g^{-1}, 100 cycles)	Zhang *et al.*[69]
4 M $Zn(BF_4)_2$-H_2O	Tetrachlorobenzoquinone	--	>2.00	~180 (220 mA g^{-1})	94% (220 mA g^{-1}, 1000 cycles)[c)]	Sun *et al.*[70]
$ZnSO_4$-H_2O/methanol	Polyaniline	16.80	>2.50	219.1 (100 mA g^{-1})	85.5% (5 A g^{-1}, 2000 cycles)	Hao *et al.*[71]
2 M $ZnSO_4$-H_2O/DMSO	MnO_2	5.00	--	267 (1 C)	~100% (10 C, 3000 cycles)	Feng *et al.*[72]
0.5 M $Zn(OTf)_2$-TEP/H_2O	V_2O_5	--	--	250 (5 A g^{-1})	~ 100% (5 A g^{-1},1000 cycles)	Liu *et al.*[73]
1 M $Zn(OTf)_2$–H_2O (30wt%)/PEG (70wt%)	V_2O_5	--	4.56	345.7 (0.5 A g^{-1})	84.3% (15 A g^{-1}, 500 cycles)	Wu *et al.*[74]
$Zn(ClO_4)_2 \cdot 6H_2O$/SN	Quinone-based polymer material (38 wt % sulfur)	5.52	>2.55	~100 (0.15 C)	85.4% (0.3 C, 3500 cycles)	Yang *et al.*[75]

(Molar ratio 1:8)						
4 m $Zn(BF_4)_2 \cdot 4.5H_2O$/EG	V_2O_5	--	--	~180 (0.2 A g^{-1})	60% (1 A g^{-1}, 800 cycles)	Han *et al.*[76]
$ZnCl_2$:acetamide:H_2O (Molar ratio 1:3:1)	Phenazine	~20	2.5	100 (1 C)	85.7% (10 C, 10 000 cycles)	Shi *et al.*[77]
7.6 m $ZnCl_2$-0.05 m $SnCl_2$-H_2O	$VOPO_4$	~81.59	>2.30	163 (1/3 C)	> 95% (1/3 C, 200 cycles)[d]	Cao *et al.*[78]
3.5 M $Mg(ClO_4)_2$ + 1 M $Zn(ClO_4)_2$-H_2O	Pyrene-4,5,9,10-tetraone	1.41[e]	---	218.7 (0.5 C)	~100% (1/3 C, 100 cycles)[e]	Sun *et al.*[79]
$Zn(ClO_4)_2 \cdot 6H_2O$-sulfolane	Polyaniline	2.00	2.53	160 (0.1 A g^{-1})	~100% (3 A g^{-1}, 2500 cycles)	Lin *et al.*[80]
Solid-state eutectic electrolytes						
2M $ZnSO_4$-4 M LiCl polyacrylamide hydrogel	$LiFePO_4$	--	--	106 (0.1 A g^{-1})	100% (0.5 A g^{-1}, 500 cycles)[f]	Zhu *et al.*[81]
$Zn(ClO_4)_2 \cdot 6H_2O$-adiponitrile hydrated gel	$Na_3V_2(PO4)_3$	~10.00	>2.60	108 (0.5 C)	~100% (10 C, 8000 cycles)	Lin *et al.*[82]
45 m $ZnCl_2$-$ZnBr_2$-1 m $Zn(OAc)_2$-H_2O Oligomers	Self-standing graphene	1.28	>1.70	605.7 (1.0 A g^{-1})	74.5% (1 A g^{-1}, 500 cycles)	Cai *et al.*[83]
$Zn(TFSI)_2$-acetamide-TiO_2	V_2O_5	3.78 x 10^{-2}	>2.60	~60 (16 mA g^{-1})	--	Qiu et al.[84]

[a] Measured at room temperature. [b] Measured at 313 K. [c] Measured at –30 °C.

[d] Measured at –50 °C. [e] Measured at –70 °C. [f] Measured at –20 °C.

3.1 Non-aqueous eutectic electrolytes

Non-aqueous eutectic electrolytes are mainly composed of organic- and Zn-based eutectic systems, no matter which composition, both act as emerging concepts in ZRFBs due to the high concentration of electroactive components. Whereas ZRFBs show limited implementation in the consumer market because of their relatively low energy density.[85] Electrolytes employed for ZRFBs typically contain redox-active materials of high molar ratio, supporting salts, and a low amount of solvents. Instead, eutectic one forms based on molecular interactions without the presence of solvents.[40] In addition, eutectic electrolytes without water contents possibly prevent problems caused by Zn dendrite growth and side reactions.[86] Analogous, some research related to Zn anodes protection and modification promotes the non-aqueous eutectic electrolytes for ZIBs[44, 87], Zn-S batteries[65], Zn-I_2 batteries[88], and Zn-Fe flow batteries[8b].

Zn-based eutectic electrolytes, constitute mixing anhydrous/hydrated Zn metal with quaternary ammonium salts (*e.g.*, ChCl) or HBDs (*e.g.*, urea, acetamide, and ethylene glycol). Here, Zn^{2+} cations participate as the redox species in the eutectic electrolyte governing H−bond interactions, coupling Halogens or organic anions (e.g., Cl^-, Br^- or $TFSI^-$) to generate eutectic electrolytes.[8b, 44, 54b] For example, Wang et al. reported $ZnCl_2$/acetamide eutectic electrolytes with concentrations ranging from 4.5 to 6.25 M for hybrid ZRFBs, where the formed $[ZnCl(acetamide)_3]^+$ of Zn–complex cations shows lower activation energy than that of the other two ($[ZnCl(acetamide)_2]^+$ and $[ZnCl(acetamide)]^+$) existed in eutectic electrolytes (**Figure 5**a). Thus, this eutectic electrolyte occurred Zn electro–stripping preferably via one main path through direct $[ZnCl(acetamide)_3]^+$ formation.[42] As mentioned above, another eutectic electrolyte of acetamide–$Zn(TFSI)_2$ present anion-containing Zn complexes ($[ZnTFSI_m(acetamide)_n]^{(2-m)+}$, m=1–2, n=1–3) that formed via the coordination between Zn^{2+} and a large portion of $TFSI^-$, which correspond to the bands' deconvolution of Raman identifying the ubiquitous presence of cation-anion coordination (as long-lived loose ion pairs). Furthermore, this complex simultaneously induces the preferential reductive decomposition of $TFSI^-$ prior to Zn deposition for a well-defined anion-derived SEI layer, stabilizing Zn anode during Zn plating/stripping (**Figure 5**b).[44]

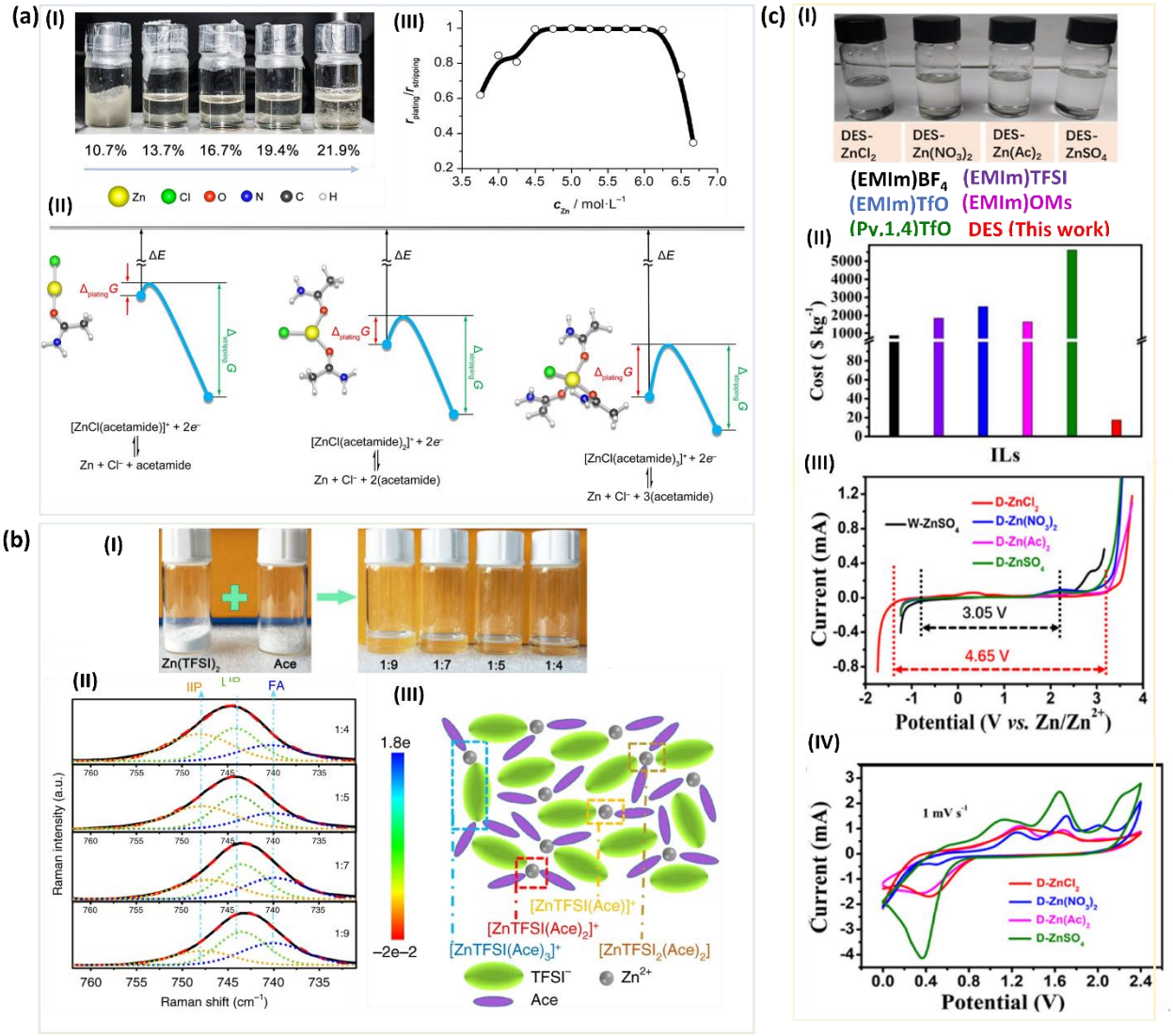

Figure 5. (a) (I) Images showing the effect of different $ZnCl_2$ molar fraction on the formation of Zn eutectic electrolytes; (II) Schematic illustration of the dissociation energy (ΔE) of Zn^{2+} complexes and activation energy of three main Zn complex cations during electroplating ($\Delta_{plating}G$) and electro–stripping ($\Delta_{stripping}G$) processes in the Zn eutectic electrolytes; (III) Electroplating/electro–stripping ratio ($r_{plating}/r_{stripping}$) versus $ZnCl_2$ concentration (C_{Zn}) at room temperature. Reproduced with permission.[42] Copyright 2018, Nature Publishing Group. (b) (I) Images of prepared $Zn(TFSI)_2$–acetamide eutectic electrolytes in molar ratio range from 1:9 to 1:4; (II) Fitted Raman spectra of different molar ratios for $Zn(TFSI)_2$–acetamide; (III) Illustration of the representative environment of active Zn species within eutectic electrolytes. Reproduced with permission.[44] Copyright 2019, Nature Publishing Group. (c) (I) Images of 1 m $ZnCl_2$, $Zn(NO_3)_2$, $Zn(Ac)_2$, and $ZnSO_4$ dissolutions in the ChCl–urea DES; (II) Cost comparison of ILs and as-prepared eutectic electrolytes; (III) ESW of different eutectic electrolytes determined by LSV curves at 10 mV s^{-1}; (IV) CV curves of Zn−S batteries in

eutectic electrolytes. Reproduced with permission.[65] Copyright 2021, American Chemistry Society.

Organic-based eutectic electrolytes, are a class of the facile eutectic system to boost the concentration of metal and organic active components given interactions effects, and additionally, an excellent exhibition of low vapor pressure and thermostability heighten practical implementation.[89] Representatively, the low-cost DES using urea and ChCl with a stoichiometric ratio of 2:1 shows good solubility for various Zn salts [*e.g.*, Zn sulfate ($ZnSO_4$), $ZnCl_2$, Zn nitrate ($Zn(NO_3)_2$), and Zn acetate ($Zn(Ac)_2$)], high ionic conductivity, and a wide electrochemical window (**Figure 5**c). The resulting eutectic electrolytes optimize the solvation structures of Zn ions in the electrolyte and allow dendrite-free Zn stripping/plating over 3920 h for Zn-S batteries.[65] Coincidentally, Cao et al. prepared a novel eutectic liquid composed of ChCl and ethylene glycol (EG) with Cerium chloride ($CeCl_3$) and $ZnCl_2$ as the active materials for positive and negative electrolytes, respectively, working for high–energy and low–cost Zn–Ce redox flow batteries.[53]

As mentioned, eutectic electrolytes can provide highly concentrated redox-active materials depending on the intermolecular interactions, and hence achieve high volumetric capacity and energy density for ZRFBs, ZIBs, and other Zn–based batteries.

3.2 Aqueous eutectic electrolytes

Eutectic electrolytes represent the tunability and compatibility with water molecules, due to the light H-bonds interruption of H_2O and tendentious reconstruction to form water-containing eutectic mixtures, particularly showing distinct advantages when applying aqueous ZIBs.[7a, 43b] Here, water induces the ion mobility through existing nanometric water channels and water-rich domains, or recently called “dynamic water presence” in the eutectic electrolytes;[61] High affinity of H-bonding structure forming between H_2O and eutectic components additionally restrict the decomposition of water, and retain equally eutectic features in a suitable eutectic regime.[31] Moreover, ice formation from water requires enlarged transformation energy to destruct the original H-bonds, which stems from kinetic ice nucleation with stacked hexagonal sequences.[90] Notably, Zn^{2+} possesses a divalent charge, a small radius, a large electric field, and strong electrostatic interactions with dipolar water molecules, in turn, causing the rearrangement of the coordination structures with water molecules and renders the melting point of resulting liquids in the formed eutectic systems.[67]

As described, Zhang *et al.* developed a 7.5m $ZnCl_2$ eutectic solution that modulated electrolyte structure, suppressed the freeze of water, and depressed the solid-liquid transition

temperature of the electrolytes from 0 to –114 °C (**Figure 6**a). Followed by this work, Zhang *et al.* continue the use of Zn salt with chaotropic anions (such as the large anion $CF_3SO_3^-$), to reduce the self-association and density of H-bonds among water molecules. After coupling with the chaotropic anion, the 2 M $Zn(CF_3SO_3)_2$ features a low freezing point of −34.1 °C and a high electrostatic potential value of –5.21 eV, and delivers a high specific capacity of 285.0 mAh g^{-1} at –30 °C with capacity retention of 81.7% after 1000 cycles when used in an aqueous ZIBs (**Figure 6**b).[69] Similar principles have been utilized with a 4M $Zn(BF_4)_2$ electrolyte that provides a very low freezing point (–122 °C) and exceptionally high ion conductivity at low temperature (1.47 mS cm^{-1} at –70 °C), demonstrating the formation of OH···F H-bonds with the breakage of those in original water molecules and exhibiting excellent electrochemical performance with a record-breaking temperature at –95 °C.[70] Beyond the direct interactions between H_2O and cations/anions, we also comprehensively summarize other fancy concepts of water-based eutectic electrolyte systems below.

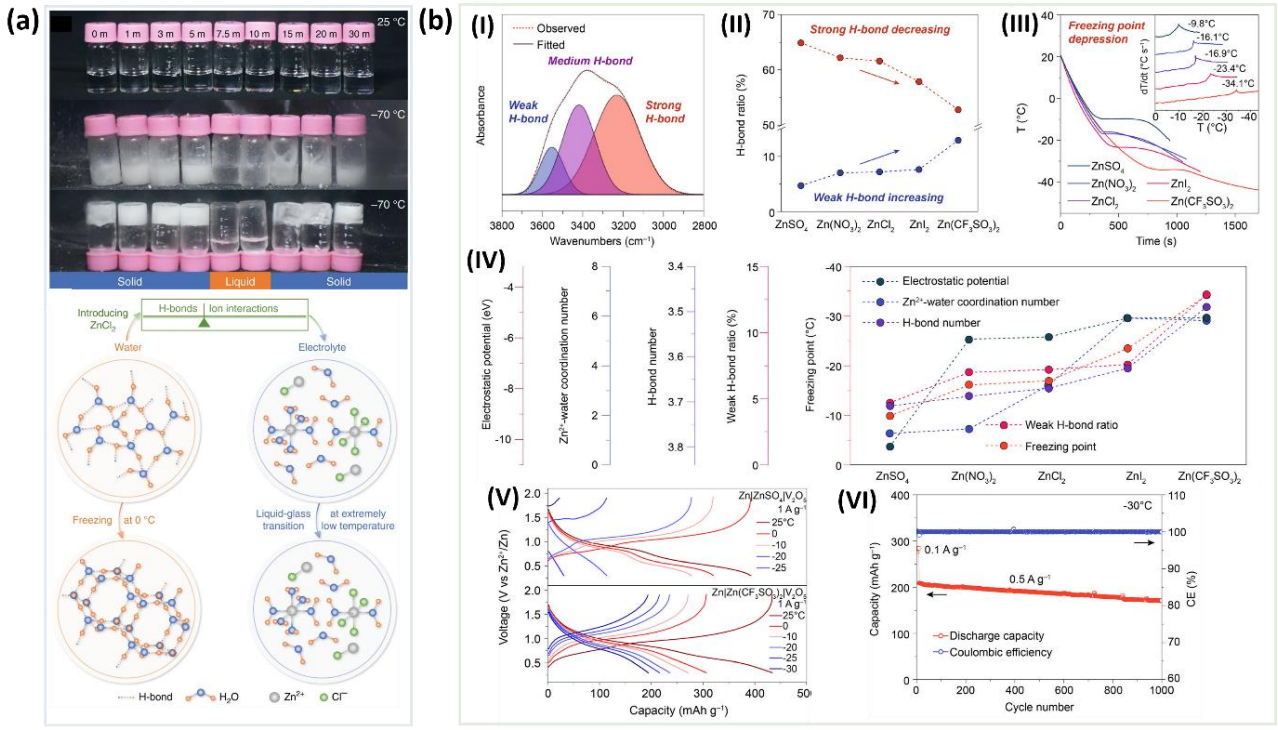

Figure 6. (a) Images of different molality electrolytes of $ZnCl_2$ at 25 and −70 °C (upper); Schematic structure evolutions of water and $ZnCl_2$ electrolyte (below). Reproduced with permission.[67] Copyright 2020, Nature Publishing Group. (b) (I) The fitted FTIR spectrum of water; (II) The calculated proportions of water with strong and weak H-bonds in the electrolytes; (III) The gradual cooling curves and the corresponding freezing points (inset) of the electrolytes; (IV) Summary of the correlations among the above-mentioned characteristics; (V) Discharge−charge voltage profiles of Zn||V_2O_5 batteries with 2 M $ZnSO_4$ and 2M $Zn(CF_3SO_3)_2$ at various temperatures; (VI) Cycling performance of the Zn|2M

$Zn(CF_3SO_3)_2|V_2O_5$ battery at –30 °C. Reproduced with permission.[69] Copyright 2021, American Chemistry Society.

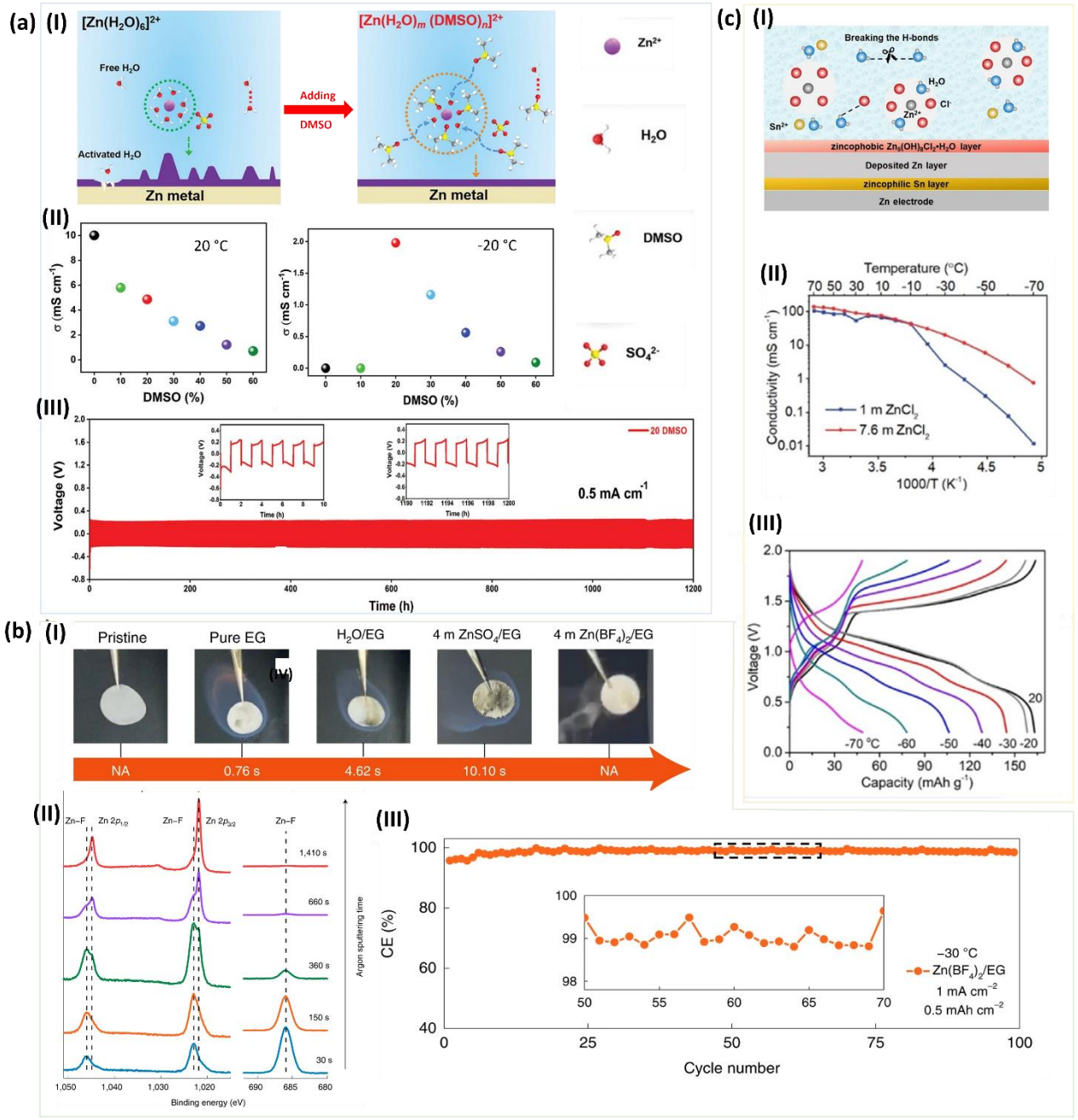

Figure 7. (a) (I) Schematics of the Zn^{2+} solvation structure and H-bonds evolution from aqueous electrolytes to various DMSO eutectic electrolytes; (II) Ionic conductivities of aqueous electrolyte and various DMSO eutectic electrolytes at 20 °C (left) and –20 °C (right); (III) Cycling performance of Zn/Zn cells with 20 DMSO eutectic electrolyte at the current density 0.5 mA cm^{-2} and areal capacity of 1 mA h cm^{-2}. Reproduced with permission.[72] Copyright 2021, WILEY-VCH. (b) (I) Ignition tests of pristine glass fiber separators, saturated with pure EG, H_2O/EG solution, 4 m $ZnSO_4$/EG solution, and 4 m $Zn(BF_4)_2$/EG solution, respectively; (II) Depth-profiling XPS spectra (Zn 2*p* and F 1*s*) of the ZnF_2 layer formed on the Zn soaked

in the 4 m $Zn(BF_4)_2$/EG electrolyte; (III) Zn plating/stripping CE in the 4 m $Zn(BF_4)_2$/EG electrolyte at 40 °C (below) and –30 °C (upper). Reproduced with permission.[91] Copyright 2021, Nature Publishing Group. (c) (I) Schematic of electrolyte and electrolyte–electrode-interphase structure; (II) Ionic conductivity at different temperatures of $ZnCl_2$ aqueous electrolytes; (III) Charge/Discharge profiles of $VOPO_4$ II Zn cells using different 7.6 m $ZnCl_2$-0.05 m $SnCl_2$ electrolytes at different temperatures. Reproduced with permission.[92] Copyright 2021, WILEY-VCH.

Co-solvent eutectic electrolytes. DMSO as a solvent additive owns a high dielectric constant and high Gutmann donor number which can preferentially solvate Zn cations and exclude water from the Zn^{2+} solvation sheath.[68] Besides, the stable reconstructed H-bonds between DMSO and H_2O dramatically lower the freezing point of the electrolyte, which significantly increases the ionic conductivity and cycling performance of aqueous Zn batteries at subzero temperatures (**Figure 7**a).[72] Alternatively, triethyl phosphate (TEP) and 1,3-dioxolane (DOL) both feature higher donor number of 26 and 21.2 kcal mol^{-1}, respectively than that of H_2O (18 kcal mol^{-1}), thus preferring to form a TEP occupied first solvation sheath and a DOL occupied second solvation around Zn^{2+}, and further inhibiting the reactivity of H_2O through strong H-bonding.[73, 93] In actuality, the function of DOL works analogously to methanol as the proposed "antisolvent" that minimizes water activity and weakens Zn^{2+} solvation. This low-cost strategy can be readily transferred to other solvents (e.g., ethanol, and 1-propanol) and promoted for its practical universality.[94] Overall, the summarized key properties of commonly used organic solvents that have been and/or potentially utilized to eutectic electrolytes are presented in **Table 2**.

Table 2. Summary of key properties of various organic solvents.

Organic solvent*	Solubility in water (g/100g)	Melting point (°C)	η (mPa s)	Dielectric constant	Donor number (kcal mol^{-1})
Dimethyl sulfoxide (DMSO)	Miscible	19.0	2.00	46.7	29.8
1,3-Dioxolane (DOL)	Miscible	-95.0	0.56	7.34	21.2
Trimethyl phosphate (TMP)	Miscible	-46.0	1.30	21.6	--
Dimethylacetamide (DMA)	Miscible	-20.0	0.95	37.8	--
Acetonitrile (CH_3CN)	Miscible	-45.0	0.34	37.5	14.1
Dimethylformamide (DMF)	Miscible	-61.0	0.80	37.0	26.5
Dimethyl carbonate (DMC)	13.9	3.0	0.59	3.1	16.0
Diethylene glycol dimethyl ether (Diglyme)	Miscible	-64	1.88	7.23	--
1,1,3,3-Tetramethylurea (TMU)	Miscible	-1.0	1.60	--	40.4

* Values are obtained from web: http://murov.info/orgsolvents.htm.

Hydrated eutectic electrolytes. The room temperature hydrate-melt electrolyte was firstly explored by Yamada et al. in the formulation of $Li(TFSI)_{0.7}(BETI)_{0.3}\cdot 2H_2O$ for high-energy-density aqueous Li batteries, in which all water molecules participate in Li^+ hydration shells while retaining fluidity.[95] The optimization of these eutectic systems can be tuned via the selection of incorporated organic salts. Still, such eutectic/H_2O systems suffer from a hydration limit that usually dictates the regime, in which the structure transits from a ‘‘water-in-eutectic’’ to a “eutectic-in-water”.[56a] Yang *et al.* originally proposed a new class of hydrated eutectic Zn electrolytes with a precise hydration level based on the simple mixing of a low-cost $Zn(ClO_4)_2\cdot 6H_2O$ (Lewis acid) and a neutral ligand succinonitrile (SN, Lewis base) (*i.e.*, these

hydrated eutectic electrolytes involve no additional water except for the crystallization one from the constituent of hydrated Zn salts). This approach successfully balances the features from both eutectic and aqueous electrolytes.[75] For comparation, Han *et al.* reported another more economical and non-flammable hydrous organic electrolyte involving a hydrated $Zn(BF_4)_2$ salt and an EG solvent, which promotes the in situ formation of a favorable ZnF_2 passivation layer to protect Zn from dendritic growth and parasitic side reactions across a wide temperature range of −30 °C to 40 °C (**Figure 7**b).[91] "Water-in-DES" (WiDES) electrolytes can be regarded as a means to artificially regulate water molecules and H-bond structures from micro-scale to macro-scale for aqueous eutectic systems. For example, a $ZnCl_2$–acetamide DES is diluted by an appropriate amount of H_2O to form $[ZnCl(acetamide)_2(H_2O)]^+$ cation complexes instead of $[ZnCl(acetamide)_3]^+$, which not only provides lower dissociation energy to promote uniform Zn nucleation, but also a means to accurately control the degree of hydration in a cost effective and simplistic manner.[77]

Salt-additives eutectic electrolytes. Inspired by WIS and WIBS electrolyte systems, adding inexpensive salt additives (such as $ZnCl_2$ and LiCl) to concentrated electrolytes has proven effectively to interrupt the H-bond network of water and increase coordinated Zn^{2+} with Cl^- rather than H_2O. Additionally, these salt additives further increase salt concentration because of high solubility that further decreases the numbers of H-bonds in water. Consequently, Cao *et al.* introduced 0.05 m Tin chloride ($SnCl_2$) additive into a 7.6 m aqueous $ZnCl_2$ eutectic electrolyte to form a zincophilic Sn layer on the current collector and a dense zincophobic $Zn_5(OH)_8Cl_2{\cdot}H_2O$ SEI to help suppress water decomposition and Zn dendrite growth. Furthermore, this additive helped to achieve a high CE of Zn plating/stripping across a wide temperature window from 20 to –70 °C. Additionally, this eutectic electrolyte delivers a high ionic conductivity of 0.8 mS cm^{-1} even at −70 °C owing to the distortion of H-bonds structures by coordinated Zn^{2+} and Cl^- (**Figure 7**c).[92]

3.3 Solid-state eutectic electrolytes

Compared with liquid electrolytes, solid-state electrolytes (SSEs) take advantage of avoiding liquid leakage/evaporation with high safety and providing sufficient mechanical strength with extended battery life, that makes them suitable for use of flexible and wearable electronic devices as for ZSSBs.[96] Meanwhile, ZSSBs require free-dendrite, non-dissolution, and non-corrosion as well when using traditional organic solvents or ILs, whether looking for more tunable, non-toxic, and low-cost alternatives could effectively prevent these issues and promote its' simple assembly feature. Until recently, reports of all-solid-state or quasi-solid-state

polymer/hydrogel electrolytes have been proposed primarily exploring water-contained eutectic mixtures as the matrix to form an anti-freezing and flexible gel or polymer eutectic electrolyte. As introduced previously, DMSO acts as a cryoprotectant that aids in the development of an aqueous electrolyte with an extremely low freezing point of −130 °C.[97] Ye *et al.* proceed the advantage of this DMSO/water eutectic mixture as a precursor solution to synthesize anti-freezing polyvinyl alcohol (PVA) hydrogel, this PVA hydrogel retains admirable flexibility and a high ionic conductivity of 1.1 S m^{-1} even at −70 °C.[98] The primary novelty of this type of solid-state eutectic electrolyte is found to stabilize the interface between the electrolyte and anode/cathode, enabling smooth Zn stripping/plating and reducing parasitic side reactions. This is thanks to the strong H-bond interactions among eutectic composition and gel/polymer network, further suppressing water reactivity and reinforcing the stability of SSEs.[82]

Interestingly, Cai *et al.* recently revealed a water-salt oligomers electrolytes (WSOEs) that formed without adding additional monomers, the super-solubility (up to 75 m) of $ZnCl_2$/$ZnBr_2$/$Zn(OAc)_2$ aqueous electrolyte is attributed to the formation of acetate-capped bridging via Br^-/$Cl^-\cdots H$ and Br^-/Cl^-/$O\cdots Zn^{2+}$ interactions. As a result, this super-soluble electrolyte exhibits a polymer-like glass transition temperature around −70 °C and enables high-performance with a reversible capacity (605.7 mAh g^{-1}) and a *CE* of 98.07% (**Figure 8**a).[83] To further improve poorly conductive of Zn^{2+} especially at room temperature in ZSSBs, Qiu *et al.* constructed a heterogeneous interface which allows Zn^{2+} percolation by inducing crystallization of tailored eutectic liquids (reported previously by organic $Zn(TFSI)_2$ salt and acetamide with an optimal molar ratio of 1:7)[75] on the Lewis acid surface of a TiO_2 nucleator, which weakens ion-association and forms interfacial Zn^{2+}-percolated channels due to high-entropy eutectic-networks and results in a solid crystal with exceptional selectivity for Zn^{2+} transport. This eutectic crystallization method creates a model artificial conducting interface for solid-state Zn-ion batteries based on eutectic solidification, leading to a high Zn^{2+} transference number ($t_{Zn^{2+}}$) of 0.64 and ionic conductivity of 5.91 x 10^{-2} mS cm^{-1} at 30 °C (**Figure 8**b).[84]

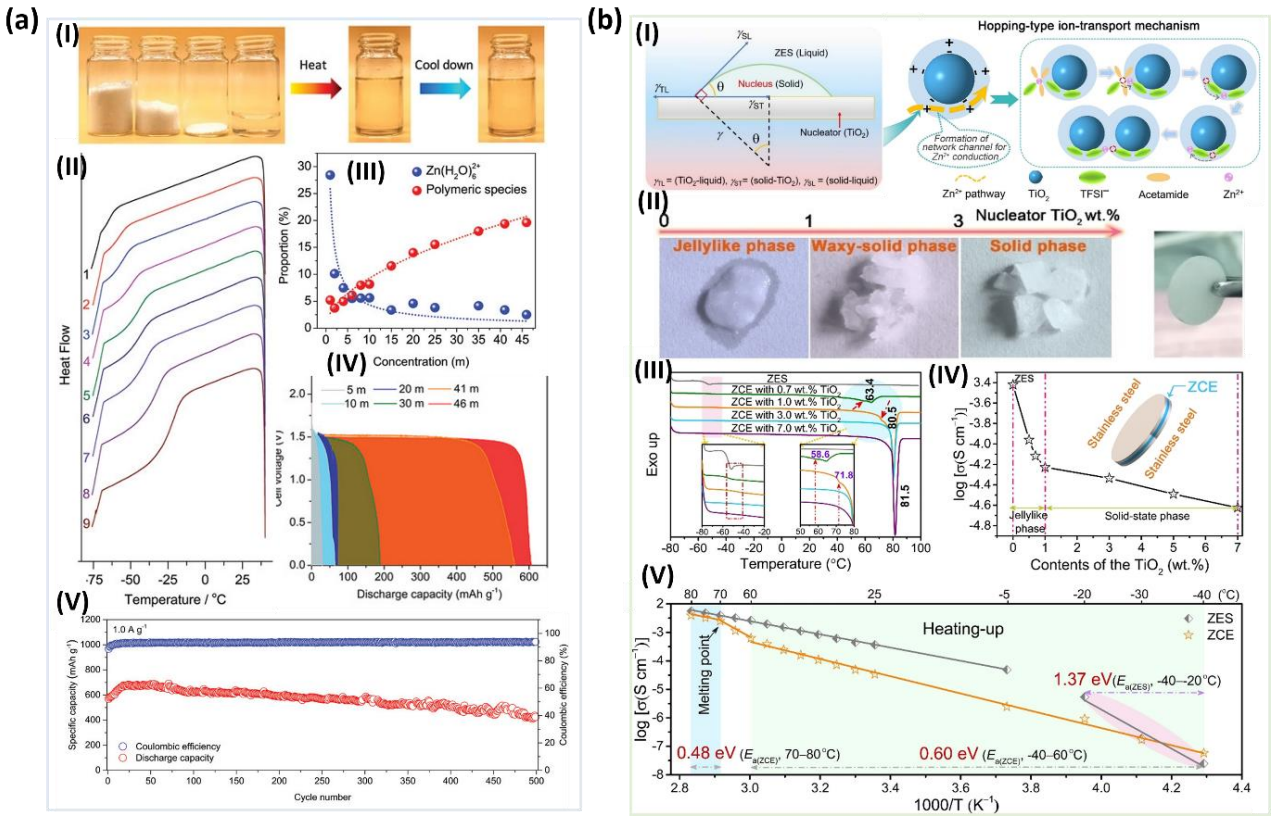

Figure 8. (a) (I) $WSOE_{45}$-1 prepared by stoichiometric amounts of $ZnCl_2$, $ZnBr_2$, $Zn(OAc)_2$, and water; (II) DSC profiles of various $WSOE_{45}$; (III) Variation trends (obtained by the integral area of separated peaks) of $[Zn(H_2O)_6]^{2+}$ and polymeric species contents in 1–46 m electrolytes; (IV) Discharge capacity of assembled dual-ion batteries using 5–46 m electrolytes; (V) Cycling stability of the dual-ion battery using $WSOE_{45}$-1 at 1 A g^{-1}. Reproduced with permission.[83] Copyright 2021, WILEY-VCH. (b) (I) Schematics of heterogeneous nucleation of Zn^{2+} conducting solid-state electrolytes (ZCEs) (right), and Zn^{2+} conducting pathways through the space-charge layers of the neighboring TiO_2 grains and the ionic hopping-type conduction mechanism (left); (II) Images of different solid samples with various wt.% of TiO_2 and the resulting bulk-solid membranes (1 wt.% TiO_2 loading); (III) DSC profiles of the pristine $Zn(TFSI)_2$-based DES and ZCEs; (IV) Ionic conductivity of ZCEs with variable TiO_2 contents at 30°C; (V) Arrhenius plots for ZCE with 1.0 wt.% TiO_2 and reference $Zn(TFSI)_2$-based DES. Reproduced with permission.[84] Copyright 2021, WILEY-VCH.

4. Eutectic electrolytes for critical RZB chemistries

Owing to the rapid evolution of Zn-based batteries in the energy storage field, many reviews have reported remarkable progress achieved to date, and challenges remained regarding RZB chemistries.[10a, 35] Among them, Zn/electrolyte interphase chemistry and ion/charge transport kinetics are considered to be two vital factors that dominate the performance, and with careful

attention, could promote the further development of RZBs. Eutectic electrolytes resemble a rising star constructively exploit interfacial strategies in RZBs from the electrolyte aspect, which no matter induce desired electrochemical properties and offer a fundamental understanding of optimizing strategies for the eutectic electrolyte.

4.1 Eutectic electrolyte/electrode interphase chemistry

The surface chemistry of an SEI is one of the most critical factors that govern the cycling life of rechargeable batteries. Eutectic electrolytes have been confirmed to be beneficial for Zn anode-related chemistry, even facing their relatively high redox potential. For example, a Zn fluoride-rich organic/inorganic hybrid SEI forms on the Zn anode from interaction with a $Zn(TFSI)_2$–acetamide eutectic electrolyte. This confirms a marked change of the $TFSI^-$ coordination environment under the intrinsic ion-association network in the present eutectic liquid.[44] Density functional theory (DFT) calculations demonstrate the altered reduction potential of interacted $TFSI^-$ with Zn^{2+} and the preferential decomposition of $TFSI^-$ over Zn^{2+} reduction leads to a $TFSI^-$-derived SEI. The open circuit-voltage decay of fully charged Zn II V_2O_5 cells illustrates the high rentability of SEI-protected Zn anode (97.8% of the original capacity) compared to bare Zn anode (68.78% of the original capacity) after discharging for 48 h (**Figure 9**a). Moreover, this rigid-flexible SEI can eliminate direct contact between the Zn anode and electrolyte, while facilitating favorable Zn^{2+} transport with a low-diffusion barrier.

Considering the applicability of implanted aqueous eutectic electrolytes, notable WiDES electrolytes composed of $ZnCl_2$-acetamide/H_2O encourage homogeneous Zn nucleation due to the fast desolvation kinetics when forming a $[ZnCl(acetamide)_2(H_2O)]^+$ cation complex. Since the water molecule has a lower energy barrier than acetamide in the step-by-step desolvation process of the Zn^{2+}-sheath, the nucleation overpotentials are reduced through modulation of the Zn^{2+} solvation structure.[77] During electrodeposition, the deposited Zn nuclei has a small size (~350 nm) and increase the number on Cu collector surface in a “WiDES” system, compared to the rather large Zn nuclei (550 nm) formation in anhydrous DES system (**Figure 9**b). Another WiDES-type electrolyte (containing ~30 mol.% H_2O in a eutectic mixture of urea/LiTFSI/$Zn(TFSI)_2$) leads to suppressed reactivity with the Zn anode from both thermodynamic and electrochemical aspects since all water molecules participate in DES's internal interaction network.[66]

Importantly, multifunctional eutectic electrolytes support protective SEI layers formation and introduce ideal cathode electrolyte interphase (CEI) layers that help to prevent the continuous decomposition of electrolyte and improve capacity. Liu *et al.* addressed cathode

dissolution mechanism by using an optimized 0.5 m Zn trifluoromethanesulfonate ($Zn(OTf)_2$)/TEP-H_2O electrolyte. The strong coordination of TEP with both Zn^{2+} and H_2O molecules results in a TEP-dominated Zn^{2+} solvation sheath, which significantly reduces the reactivity of H_2O with V_2O_5 cathode. This $Zn(OTf)_2$/TEP-H_2O electrolyte can optimize the cycling stability of oxide-based cathodes that usually suffer from structural disintegration and slow vanadium dissolution at low rates in aqueous electrolytes.[3b] These improvements inhibit of cathode dissolution and host roles of V_2O_5 in allowing Zn^{2+} ions to undergo highly reversible reactions (**Figure 9**c). Moreover, the TEP-dominated solvation structure leads to a robust polymeric-inorganic SEI on Zn anode, effectively avoiding parasitic water reaction and dendrite growth.[73] As discussed above, the low-cost hydrous organic electrolyte of 4 m hydrated $Zn(BF_4)_2$-EG in Zn II V_2O_5 full cells presents a protective effect for cycling stability at both high and low current densities, given the fact that eutectic electrolytes even involved with water could show high compatibility with cathode materials.[91]

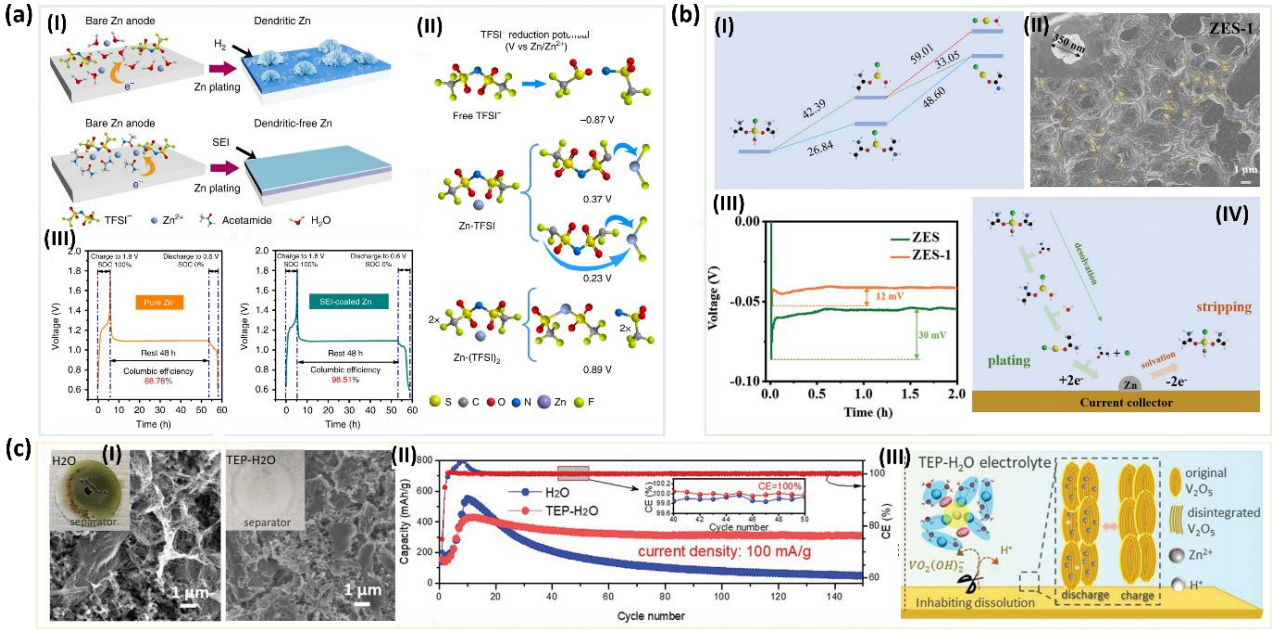

Figure 9. (a) (I) Schematics of Zn dendrite growth along with H_2 evolution observed in 1 M $Zn(TFSI)_2$ (upper) and SEI-regulated uniform Zn deposition in $Zn(TFSI)_2$–acetamide (below); (II) DFT calculations for reduction potentials of various cation-anion complex; (III) The Zn II V_2O_5 cells in 1 M $Zn(TFSI)_2$ using pure Zn anode (left) and SEI-coated Zn anode (right) were fully charged to 1.8 V at 20 mA g^{-1} (based on active materials of cathode), respectively, then discharged after 48 h. Reproduced with permission.[44] Copyright 2019, Nature Publishing Group. (b) (I) Diagram of the energy barriers (kcal mol^{-1}) during the step-by-step desolvation process of $[ZnCl(acetamide)_2(H_2O)]^+$ cation complex; (II) SEM images of Zn nuclei deposited on the Cu collector at 0.1 mA cm^{-2} with the an area capacity of 0.01 mA h cm^{-2} in WIDES

electrolytes; (III) Nucleation overpotentials at 0.1 mA cm^{-2} using Zn/Cu cells in WIDES and DES electrolytes; (IV) Schematic diagram of desolvation and solvation steps of Zn^{2+} during Zn plating/stripping process in the WIDES electrolytes. Reproduced with permission.[77] Copyright 2021, WILEY-VCH. (c) (I) SEM images of the cycled V_2O_5 electrodes and photographs of the separators (insets) in $Zn(OTf)_2$-H_2O (left) and $Zn(OTf)_2$/TEP-H_2O (right) electrolytes; (II) the cycling performance of V_2O_5 electrodes in both electrolytes under low current rates; (III) Schematic illustration of the effects of $Zn(OTf)_2$/TEP-H_2O electrolytes on V_2O_5 electrode during the electrochemical reactions. Reproduced with permission.[73] Copyright 2021, WILEY-VCH.

In general, interphase chemistry in RZBs can be synergistically regulated *via* the solvation structure with low dissociation energy and molecular complex structure with H-bond interactions in eutectic electrolytes, which eventually determines the composition and stability of eutectic electrolyte/electrode interphases through eutectic effects on deposition potential and the corresponding deposition sequence.

4.2 Ions/charges transport kinetics

Corresponding to the discussion of interphase chemistry in Zn batteries, stable and fast kinetics of ions and charges through electrodes determine further performance such as long cycling life at severe working conditions. From the view of electrolytes modification, many strategies regarding cationic/anionic chemistry[49], ion interaction regulation[99], and additive sorts[100] have addressed numerous attentions. Recently, Gao et al. shared their points for a fundamental understanding of anionic chemistry and effects on Zn batteries. In contrast with cationic one, proposing possibly the intercalation of anions into the electrode lattice structure.[101] However, anionic chemistry lacks systematically theoretical guidelines, such as the irreversible structural transformation of the anionic framework in the electrode crystal lattice likely resulting in rapid capacity decay Thus the demand for the rational design of anionic chemistry-based electrodes further limits its application. Meanwhile, the fundamental understanding of ion and charges diffusion kinetics guides future directions in developing eutectic electrolytes for suitable RZBs.

As demonstrated above, a chaotropic anion of $CF_3SO_3^-$ coupling with Zn cation formed eutectic liquid at low concentration delivers the fast-kinetics of an amorphous V_2O_5 cathode and good low-temperature performance in Zn||V_2O_5 batteries.[69] For electrolyte design, several anions (*i.e.*, SO_4^{2-}, NO_3^-, Cl^-, and I^-) and the corresponding Zn-based electrolytes have been investigated using DFT calculations, showing the order of the anions $SO_4^{2-} < NO_3^- < Cl^- < I^- < CF_3SO_3^-$ in terms of the ESP values. For electrodes, DFT calculations display the desolvation

process of rate-determining step during discharging/charging at low temperatures, where a high energy barrier of 289.3 kcal mol^{-1} has been required by $[Zn(H_2O)_6]^{2+}$. While inorganic V_2O_5 cathodes exhibit flexible insertion pathways that, benefits the synergetic insertion of Zn^{2+} and H_2O endowing fast discharge−charge kinetics. Moreover, the electrochemical reactions of $Zn||V_2O_5$ battery utilizing eutectic electrolytes suggest simultaneous domination of ionic diffusion and pseudocapacitance, which significantly contribute to fast ionic diffusion kinetics and excellent low-temperature performance *(i.e.*, remaining the ionic conductivity of 4.47 mS cm^{-1} at −30 °C). Compared to the inorganic cathode (V_2O_5), the use of polyaniline (PANI) as an organic cathode material relies on the redox mechanism of the benzene/quinone structure transformation and the corresponding ions compensation provides potential for the construction of low-temperature Zn batteries.[102] When cooperating with the 7.5 m $ZnCl_2$ eutectic electrolyte in Zn II PANI cells, the PANI cathode maintains charge balance by $H^+/ZnCl^+$ adsorption and $(H_2O)_2Cl_4^{2-}$desorption with the internal structure transformation, which possesses the same redox mechanism across normal and low temperature owing to the slow mass transfer kinetics that reveal the weakened redox peaks and enlarged electrochemical polarization. Practically exploring the relationship across $ZnCl_2$ concentration ($C_{Zn^{2+}}$) electrolyte structure, $ZnCl_2$-based aqueous electrolytes present reduced solid-liquid transition temperatures with increased $C_{Zn^{2+}}$ indicating breakage of H-bonds interactions and enhancement of ion interactions. Therefore, $ZnCl_2$ electrolytes with 7.5 m holds the eutectic point of –114 °C and exhibit a high ionic conductivity of 1.79 mS cm^{-1} at –60 °C. [67]

Based on the importance of compatibility between the electrolyte and cathode/anode, advanced eutectic electrolytes have partially prepared for reasonable and design and accelerated adaption for tunable electrodes, further widening the application of RZBs considering diverse environmental factors.

5. Summary and Outlook

In this review, we comprehensively illustrate the fundamentals of eutectic electrolytes including a well-defined discussion of the definition, composition, formation mechanism, and detection technique across utilization in RZB applications. In particular, we firstly present a specific classification of eutectic electrolytes categories integrating recent progress in the development of Zn-based batteries. In the subsequent section, the discussion of eutectic electrolytes evaluating the effect of ions/charge transport kinetics and electrolyte/electrode interphase displays functional insights for Zn battery chemistry. Compared to conventional electrolyte systems, eutectic electrolytes take advantage of high ionic conductivity, thermal stability,

nonflammability, nontoxicity, and low cost, all of which validates eutectic-type mixtures as a suitable and promising green material for constructing affordable, safe, and commercializable RZBs. However, eutectic electrolytes as a rising star still receive limited research attention at the current stage, but not without already achieving some vital progress. Therefore, some of following challenges and future efforts summarized below should guide future exploration towards the development of suitable eutectic electrolyte systems for RZBs (**Figure 10)**.

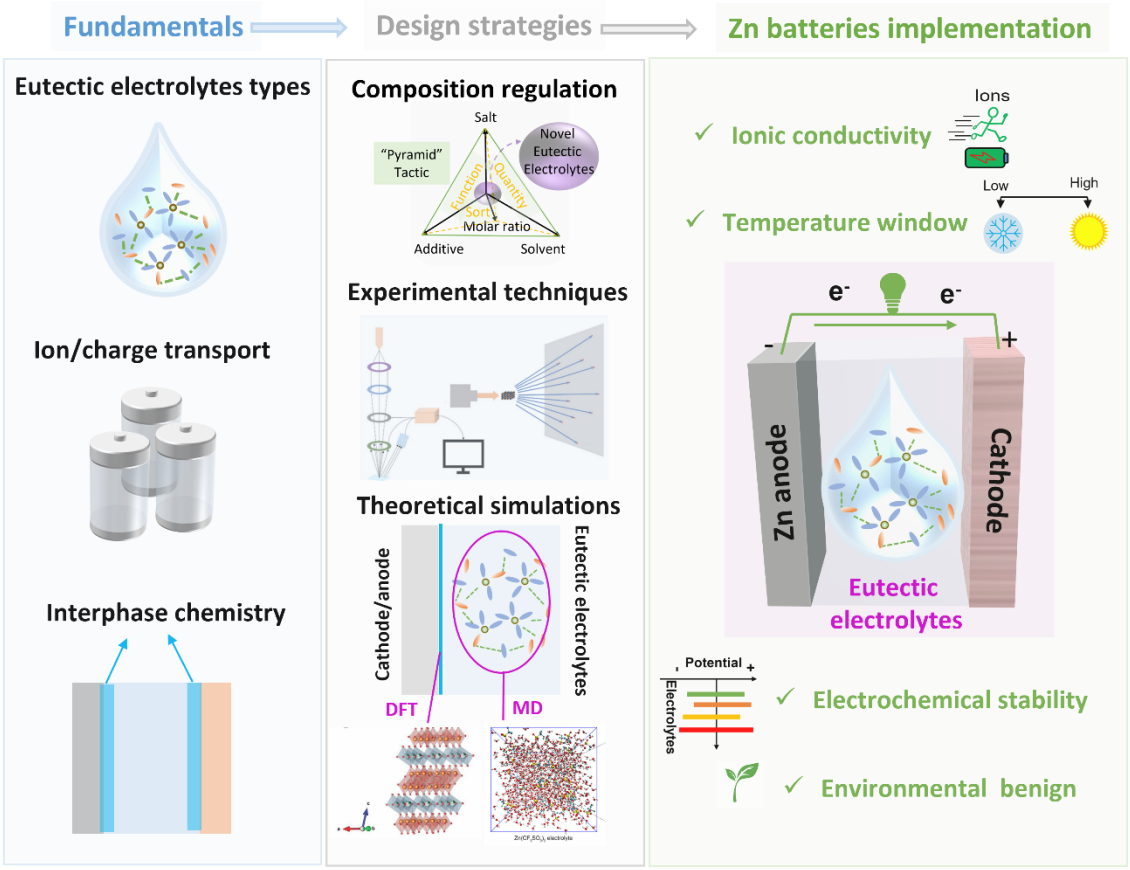

Figure 10. Summary and perspectives of eutectic electrolytes for RZBs.

Challenges.

Initially, the ionic conductivity of liquid eutectic systems still needs improvements. More specifically, this is crucial for those with organic Zn salts and HBDs composed by Lewis acid-base interactions that normally denote large size characteristics of ions and relatively free volume resulting in undesirable viscosity at room temperature. Although some examples have demonstrated that eutectic electrolytes are compatible with metal-oxide, particularly those with flexible structure transformation (*i.e.*, V_2O_5) cause a favorable combination of organic electrode materials and eutectic electrolytes. Furthermore, the high concentration feature of eutectic systems affecting the activity and stability of the involved Zn redox reactions still needs further exploration. Additionally, many compositions of eutectics are in a state of less-investigated and -employed, such as eutectic ILs prepared by mixing two kinds of ILs have significantly lower

freezing points than that of single IL, also resulting in significantly enhanced low-temperature ionic conductivity. Finally, practical cases that implement eutectic electrolytes in Zn-based batteries usually singularly focus on the excellence in low-temperature performance, while high-temperature behavior above 60 °C and relative battery chemistry need to be reported with equal importance.

Perspectives.

(1) As stated above, future work should be dedicated to composition selection, ratio regulation, and additive sorting for eutectic electrolytes design and modification. In this review, we propose the "Pyramid" tactic that delivers muti-dimensional spaces devoted to the distinct thinking of novel eutectic systems, which performs as the efficient guidelines for the emerging demand of high energy/power, non-toxic, and low-cost RZBs.

(2) Interestingly, few amounts of water existing in eutectic systems or so-called "water-in-eutectics" can overcome their significant drawbacks with preservation of appealing properties in the original ones, the dilution regime tuned with stoichiometric amounts distorts the tetrahedral structure of water when incorporating *via* new-formed H-bonds.[55a] Additionally, water molecules found with vibrational and rotational properties facilitate the design of solvation structures of eutectic electrolytes.[61] Thus water-induced eutectic systems can expand the vision and direction for optimized exploitation of eutectic electrolytes.

(3) The formation of eutectic ILs finally results in a combination of ions interacting alternatively with all the possible counterions.[103] Accordingly, the correlation between the ionic interactions of ILs and H-bonds of DESs possibly appears to occur transitioning from the one to the other one,[104] which partially endows the performance of existing ILs/DESs and the possibility for proposing modern and ecofriendly eutectic electrolytes.

(4) Eutectic electrolytes can also be designed particularly from aspects of artificial SEI/CEI formation, while the key is to find superior coupling of unique ingredients which assists strong H-bonding between them. Apart from that, a symmetrical analysis regarding the compatibility between the eutectic electrolytes and electrode materials should be investigated. To achieve this, supports from advanced techniques and working mechanisms direct compatibilities between the utility of eutectic electrolytes and the performance of Zn-based batteries.

(5) Specifically, relevant solid-liquid state phase diagram provides preferent formulation and information regarding temperature and composition range. In terms of rational optimization, adding additives like organic solvents with high dielectric number can effectively reduce ions size and the viscosity for increased ionic conductivity. Complementarily, to deal with demands

for high electrochemical stability, choosing one with excellent thermal/electrochemical stability at high temperatures promises to achieve better RZBs with enhanced ion transport kinetics.

(6) Beneficially, theoretical simulations including modeling (molecular dynamics, MD) and calculation (DFT) along with ex-situ or in-situ/operando characterizations help further investigate the coordination geometries and formation mechanism of eutectic systems at the molecular level.

(7) Ultimately, more efforts should be invested in combing high-performance eutectic electrolytes with various RZB prototypes, such as pouch cell assembly and/or battery packs for electric vehicles, pursuing high energy, low-cost, and safety involved full-scale prototypes of Zn-based EES devices.

Overall, eutectic electrolytes have shown significant potential opening new avenues for advanced Zn-based batteries, particularly regarding economical, feasible, and environmentally benign aspects. Notably, we believe the versatile types and functionalities of eutectic electrolytes efficiently bridge the accelerated development of other energy storage devices (*i.e.*, sodium, calcium, aluminum, and magnesium-based batteries/SCs) in the future.[89, 105]

Acknowledgements

This work was supported by the Natural Sciences and Engineering Research Council of Canada (NSERC), Canada Foundation for Innovation (CFI), B.C. Knowledge Development Fund (BCKDF), and the University of British Columbia (UBC).

Received: (will be filled in by the editorial staff)
Revised: (will be filled in by the editorial staff)
Published online: (will be filled in by the editorial staff)

References

[1] a) H. K. Bruce Dunn, Jean-Marie Tarascon, *Science* **2011**, *334*, 928-935; b) T. C. Johnstone, G. Wee and D. W. Stephan, *Angew. Chem. Int. Ed.* **2018**, *57*, 5881-5884.
[2] P. Canepa, G. Sai Gautam, D. C. Hannah, R. Malik, M. Liu, K. G. Gallagher, K. A. Persson and G. Ceder, *Chem. Rev.* **2017**, *117*, 4287-4341.
[3] a) Z. Yang, J. Zhang, M. C. Kintner-Meyer, X. Lu, D. Choi, J. P. Lemmon and J. Liu, *Chem. Rev.* **2011**, *111*, 3577-3613; b) L. E. Blanc, D. Kundu and L. F. Nazar, *Joule* **2020**, *4*, 771-799.
[4] Z. Liu, Y. Huang, Y. Huang, Q. Yang, X. Li, Z. Huang and C. Zhi, *Chem. Soc. Rev.* **2020**, *49*, 180-232.
[5] W. Z. Dongliang Chao, Fangxi Xie, Chao Ye, Huan Li, Mietek Jaroniec, Shi-Zhang Qiao, *Sci. Adv.* **2020**, *6*, eaba4098.

[6] a) M. Song, H. Tan, D. Chao and H. J. Fan, *Adv. Funct. Mater.* **2018**, *28*, 1802564; b) H. Li, L. Ma, C. Han, Z. Wang, Z. Liu, Z. Tang and C. Zhi, *Nano Energy* **2019**, *62*, 550-587.
[7] a) C. Liu, X. Xie, B. Lu, J. Zhou and S. Liang, *ACS Energy Lett.* **2021**, *6*, 1015-1033; b) Y. Shi, Y. Chen, L. Shi, K. Wang, B. Wang, L. Li, Y. Ma, Y. Li, Z. Sun, W. Ali and S. Ding, *Small* **2020**, *16*, e2000730.
[8] a) G. Li, W. Chen, H. Zhang, Y. Gong, F. Shi, J. Wang, R. Zhang, G. Chen, Y. Jin, T. Wu, Z. Tang and Y. Cui, *Adv. Energy Mater.* **2020**, *10*, 1902085; b) M. Yang, Z. Xu, W. Xiang, H. Xu, M. Ding, L. Li, A. Tang, R. Gao, G. Zhou and C. Jia, *Energy Storage Mater.* **2022**, *44*, 433-440.
[9] a) C. Han, T. Zhang, J. Li, B. Li and Z. Lin, *Nano Energy* **2020**, *77*, 105165; b) L. Ma, S. Chen, N. Li, Z. Liu, Z. Tang, J. A. Zapien, S. Chen, J. Fan and C. Zhi, *Adv. Mater.* **2020**, *32*, e1908121; c) G. Shim, M. X. Tran, G. Liu, D. Byun and J. K. Lee, *Energy Storage Mater.* **2021**, *35*, 739-749.
[10] a) Y. Liu, X. Lu, F. Lai, T. Liu, P. R. Shearing, I. P. Parkin, G. He and D. J. L. Brett, *Joule* **2021**, *5*, 2845-2903; b) W. Kao‐ian, A. A. Mohamad, W. R. Liu, R. Pornprasertsuk, S. Siwamogsatham and S. Kheawhom, *Batteries & Supercaps* **2022**, e202100361.
[11] J. Cao, D. Zhang, X. Zhang, Z. Zeng, J. Qin and Y. Huang, *Energy & Environmental Science* **2022**, *15*, 499-528.
[12] J. F. Parker, C. N. Chervin, I. R. Pala, M. Machler, M. F. Burz, J. W. Long and D. R. Rolison, *Science* **2017**, *356*, 415–418.
[13] F. Wang, O. Borodin, T. Gao, X. Fan, W. Sun, F. Han, A. Faraone, J. A. Dura, K. Xu and C. Wang, *Nat. Mater.* **2018**, *17*, 543-549.
[14] a) Z. Ye, Z. Cao, M. O. Lam Chee, P. Dong, P. M. Ajayan, J. Shen and M. Ye, *Energy Storage Materials* **2020**, *32*, 290-305; b) M. E. Di Pietro and A. Mele, *J. Mol. Liq.* **2021**, *338*, 116597; c) G. A. Giffin, *J. Mater. Chem. A* **2016**, *4*, 13378-13389.
[15] L. Suo, Y. S. Hu, H. Li, M. Armand and L. Chen, *Nat. Comm.* **2013**, *4*, 1481.
[16] L. Suo, O. Borodin, T. Gao, M. Olguin, J. Ho, X. Fan, C. Luo, C. Wang and K. Xu, *Science* **2015**, *350*, 938-943.
[17] a) L. Zhang, I. A. Rodríguez‐Pérez, H. Jiang, C. Zhang, D. P. Leonard, Q. Guo, W. Wang, S. Han, L. Wang and X. Ji, *Adv. Funct. Mater.* **2019**, *29*, 1902653; b) G. Yang, J. Huang, X. Wan, B. Liu, Y. Zhu, J. Wang, O. Fontaine, S. Luo, P. Hiralal, Y. Guo and H. Zhou, *EcoMat* **2022**, e12165; c) D. Chen, M. Lu, D. Cai, H. Yang and W. Han, *Journal of Energy Chemistry* **2021**, *54*, 712-726.
[18] a) S. Chen, R. Lan, J. Humphreys and S. Tao, *Energy Storage Mater.* **2020**, *28*, 205-215; b) X. Song, H. He, M. H. Aboonasr Shiraz, H. Zhu, A. Khosrozadeh and J. Liu, *Chem. Comm.* **2021**, *57*, 1246-1249.
[19] L. Droguet, A. Grimaud, O. Fontaine and J. M. Tarascon, *Adv. Energy Mater.* **2020**, *10*, 2002440.
[20] A. P. Abbott, G. Capper, D. L. Davies, H. L. Munro, R. K. Rasheed and V. Tambyrajah, *Chem. Comm.* **2001**, 2010-2011.
[21] Z. Liu, T. Cui, T. Lu, M. Shapouri Ghazvini and F. Endres, *J. Phys. Chem. C* **2016**, *120*, 20224-20231.
[22] a) M. Forsyth, L. Porcarelli, X. Wang, N. Goujon and D. Mecerreyes, *Acc. Chem. Res.* **2019**, *52*, 686-694; b) W. Zhou, M. Zhang, X. Kong, W. Huang and Q. Zhang, *Adv. Sci.* **2021**, *8*, 2004490.
[23] A. P. Abbott, D. Boothby, G. Capper, D. L. Davies and R. K. Rasheed, *J. Am. Chem. Soc.* **2004**, *126*, 9142–9147.
[24] J. Wu, Q. Liang, X. Yu, Q. F. Lü, L. Ma, X. Qin, G. Chen and B. Li, *Adv. Funct. Mater.* **2021**, *31*.
[25] X. Lu, R. J. Jimenez-Rioboo, D. Leech, M. C. Gutierrez, M. L. Ferrer and F. Del Monte, *ACS Appl. Mater. Interfaces* **2020**, *12*, 29181-29193.

[26] X. Lu, J. M. Vicent-Luna, S. Calero, R. M. Madero-Castro, M. C. Gutiérrez, M. L. Ferrer and F. del Monte, *Energy Storage Mater.* **2021**, *40*, 368-385.
[27] M. R. Lukatskaya, J. I. Feldblyum, D. G. Mackanic, F. Lissel, D. L. Michels, Y. Cui and Z. Bao, *Energy Environ. Sci.* **2018**, *11*, 2876-2883.
[28] J. Xu, X. Ji, J. Zhang, C. Yang, P. Wang, S. Liu, K. Ludwig, F. Chen, P. Kofinas and C. Wang, *Nature Energy* **2022**, https://doi.org/10.1038/s41560-41021-00977-41565.
[29] Z. Wang, Y. Xu, J. Peng, M. Ou, P. Wei, C. Fang, Q. Li, J. Huang, J. Han and Y. Huang, *Small* **2021**, *17*, e2101650.
[30] T. Mandai, K. Yoshida, K. Ueno, K. Dokko and M. Watanabe, *Phys. Chem. Chem. Phys.* **2014**, *16*, 8761-8772.
[31] Q. Zhang, K. De Oliveira Vigier, S. Royer and F. Jerome, *Chem. Soc. Rev.* **2012**, *41*, 7108-7146.
[32] E. L. Smith, A. P. Abbott and K. S. Ryder, *Chem. Rev.* **2014**, *114*, 11060-11082.
[33] a) A. P. Abbott, *Chemphyschem* **2004**, *5*, 1242-1246; b) Andrew P. Abbott, Robert C. Harris and K. S. Ryder, **2007**, *111*, 4910-4913.
[34] B. B. Hansen, S. Spittle, B. Chen, D. Poe, Y. Zhang, J. M. Klein, A. Horton, L. Adhikari, T. Zelovich, B. W. Doherty, B. Gurkan, E. J. Maginn, A. Ragauskas, M. Dadmun, T. A. Zawodzinski, G. A. Baker, M. E. Tuckerman, R. F. Savinell and J. R. Sangoro, *Chem. Rev.* **2021**, *121*, 1232-1285.
[35] L. Yuan, J. Hao, C.-C. Kao, C. Wu, H.-K. Liu, S.-X. Dou and S.-Z. Qiao, *Energy Environ. Sci.* **2021**, *14*, 5669-5689.
[36] A. P. Abbott, G. Capper, D. L. Davies, R. K. Rasheed and V. Tambyrajah, *Chem. Comm.* **2003**, 70-71.
[37] Andrew P. Abbott, Glen Capper, David L. Davies, Katy J. McKenzie and S. U. Obi, *J. Chem. Eng. Data* **2006**, *51*, 1280–1282.
[38] A. P. Abbott, J. C. Barron, K. S. Ryder and D. Wilson, *Chem. Eur. J.* **2007**, *13*, 6495-6501.
[39] D. O. Abranches, M. A. R. Martins, L. P. Silva, N. Schaeffer, S. P. Pinho and J. A. P. Coutinho, *Chem. Comm.* **2019**, *55*, 10253-10256.
[40] C. Zhang, L. Zhang and G. Yu, *Acc. Chem. Res.* **2020**, *53*, 1648-1659.
[41] A. M. Navarro-Suárez and P. Johansson, *J. Electrochem. Soc.* **2020**, *167*.
[42] Y. Wang, Z. Niu, Q. Zheng, C. Zhang, J. Ye, G. Dai, Y. Zhao and X. Zhang, *Sci. Rep.* **2018**, *8*, 5740.
[43] a) L. Huang, N. Huo, Y. Li, H. Chen, J. Yang, Z. Wei, J. Li and S. S. Li, *J. Phys. Chem. Lett.* **2015**, *6*, 2483-2488; b) L. Geng, X. Wang, K. Han, P. Hu, L. Zhou, Y. Zhao, W. Luo and L. Mai, *ACS Energy Lett.* **2022**, *7*, 247-260.
[44] H. Qiu, X. Du, J. Zhao, Y. Wang, J. Ju, Z. Chen, Z. Hu, D. Yan, X. Zhou and G. Cui, *Nat. Comm.* **2019**, *10*, 5374.
[45] H. Ogawa and H. Mori, *Phys. Chem. Chem. Phys.* **2020**, *22*, 8853-8863.
[46] a) C. Zhong, Y. Deng, W. Hu, J. Qiao, L. Zhang and J. Zhang, *Chem. Soc. Rev.* **2015**, *44*, 7484-7539; b) M. Li, C. Wang, Z. Chen, K. Xu and J. Lu, *Chem. Rev.* **2020**, *120*, 6783-6819.
[47] a) T. Zhang, Y. Tang, S. Guo, X. Cao, A. Pan, G. Fang, J. Zhou and S. Liang, *Energy Environ. Sci.* **2020**, *13*, 4625-4665; b) T. El Achkar, H. Greige-Gerges and S. Fourmentin, *Environ. Chemi. Lett.* **2021**, *19*, 3397-3408.
[48] a) J. Chen, A. Naveed, Y. Nuli, J. Yang and J. Wang, *Energy Storage Mater.* **2020**, *31*, 382-400; b) J. Xie, Z. Liang and Y. C. Lu, *Nat. Mater.* **2020**, *19*, 1006-1011; c) Y. Yamada, J. Wang, S. Ko, E. Watanabe and A. Yamada, *Nat. Energy* **2019**, *4*, 269-280.
[49] N. Zhang, X. Chen, M. Yu, Z. Niu, F. Cheng and J. Chen, *Chem. Soc. Rev.* **2020**, *49*, 4203-4219.

[50] E. Arunan, G. R. Desiraju, R. A. Klein, J. Sadlej, S. Scheiner, I. Alkorta, D. C. Clary, R. H. Crabtree, J. J. Dannenberg, P. Hobza, H. G. Kjaergaard, A. C. Legon, B. Mennucci and D. J. Nesbitt, *Pure App. Chemi.* **2011**, *83*, 1637-1641.
[51] D. Gardiner, P. Graves and H. Bowley, *Springer-Verlag* **1989**.
[52] R. Salzer, *Anal. Bioanal. Chem* **2008**, *391*, 2379-2380.
[53] X. Cao, S. Wang and X. Xue, *ChemSusChem* **2021**, *14*, 1747-1755.
[54] a) K. Kremer and S. F., *Springer-Verlag* **2003**; b) M. Ulaganathan, S. Suresh, K. Mariyappan, P. Periasamy and R. Pitchai, *ACS Sustainable Chem. Eng.* **2019**, *7*, 6053-6060; c) X. Lu, J. M. Vicent-Luna, S. Calero, M. J. Roldan-Ruiz, R. Jimenez, M. L. Ferrer, M. C. Gutierrez and F. Del Monte, *ChemSusChem* **2020**, *13*, 5983-5995.
[55] a) N. López-Salas, J. M. Vicent-Luna, S. Imberti, E. Posada, M. J. Roldán, J. A. Anta, S. R. G. Balestra, R. M. Madero Castro, S. Calero, R. J. Jiménez-Riobóo, M. C. Gutiérrez, M. L. Ferrer and F. del Monte, *ACS Sustainable Chem. Eng.* **2019**, *7*, 17565-17573; b) N. López-Salas, J. M. Vicent-Luna, E. Posada, S. Imberti, R. M. Madero-Castro, S. Calero, C. O. Ania, R. J. Jiménez-Riobóo, M. C. Gutiérrez, M. L. Ferrer and F. del Monte, *ACS Sustainable Chem. Eng.* **2020**, *8*, 12120-12131.
[56] a) O. S. Hammond, D. T. Bowron and K. J. Edler, *Angew. Chem. Int. Ed.* **2017**, *56*, 9782-9785; b) C. F. Araujo, J. A. P. Coutinho, M. M. Nolasco, S. F. Parker, P. J. A. Ribeiro-Claro, S. Rudic, B. I. G. Soares and P. D. Vaz, *Phys. Chem. Chem. Phys.* **2017**, *19*, 17998-18009.
[57] V. S. Raghuwanshi, M. Ochmann, A. Hoell, F. Polzer and K. Rademann, *Langmuir* **2014**, *30*, 6038-6046.
[58] S. J. Bryant, R. Atkin and G. G. Warr, *Langmuir* **2017**, *33*, 6878-6884.
[59] a) T. Wang, Z. Tian, Z. You, Z. Li, H. Cheng, W. Li, Y. Yang, Y. Zhou, Q. Zhong and Y. Lai, *Energy Storage Mater.* **2022**, *45*, 24-32; b) X. Liu, S.-C. Lee, S. Seifer, R. E. Winans, L. Cheng, Y. Z and T. Li, *Energy Storage Mater.* **2021**.
[60] a) F. Kremer, *J. Non-Cryst. Solids* **2002**, *305*, 1-9; b) K. Asami, *Prog. Polym. Sci.* **2002**, *27* 1617–1659.
[61] J. Kim, B. Koo, J. Lim, J. Jeon, C. Lim, H. Lee, K. Kwak and M. Cho, *ACS Energy Lett.* **2022**, *7*, 189-196.
[62] a) M. Francisco, A. van den Bruinhorst and M. C. Kroon, *Green Chem.* **2012**, *14*; b) R. Craveiro, I. Aroso, V. Flammia, T. Carvalho, M. T. Viciosa, M. Dionísio, S. Barreiros, R. L. Reis, A. R. C. Duarte and A. Paiva, *J. Mol. Liq.* **2016**, *215*, 534-540.
[63] S. Ravula, N. E. Larm, M. A. Mottaleb, M. P. Heitz and G. A. Baker, *Chem. Engineering* **2019**, *3*, 42.
[64] W. Kao-ian, R. Pornprasertsuk, P. Thamyongkit, T. Maiyalagan and S. Kheawhom, *J. Electrochem. Soc.* **2019**, *166*, A1063-A1069.
[65] M. Cui, J. Fei, F. Mo, H. Lei and Y. Huang, *ACS Appl. Mater. Interfaces* **2021**, *13*, 54981-54989.
[66] J. Zhao, J. Zhang, W. Yang, B. Chen, Z. Zhao, H. Qiu, S. Dong, X. Zhou, G. Cui and L. Chen, *Nano Energy* **2019**, *57*, 625-634.
[67] Q. Zhang, Y. Ma, Y. Lu, L. Li, F. Wan, K. Zhang and J. Chen, *Nat. Comm.* **2020**, *11*, 4463.
[68] L. Cao, D. Li, E. Hu, J. Xu, T. Deng, L. Ma, Y. Wang, X. Q. Yang and C. Wang, *J. Am. Chem. Soc.* **2020**, *142*, 21404-21409.
[69] Q. Zhang, K. Xia, Y. Ma, Y. Lu, L. Li, J. Liang, S. Chou and J. Chen, *ACS Energy Lett.* **2021**, *6*, 2704-2712.
[70] T. Sun, X. Yuan, K. Wang, S. Zheng, J. Shi, Q. Zhang, W. Cai, J. Liang and Z. Tao, *J. Mater. Chem. A* **2021**, *9*, 7042-7047.
[71] J. Hao, L. Yuan, C. Ye, D. Chao, K. Davey, Z. Guo and S. Z. Qiao, *Angew. Chem. Int. Ed.* **2021**, *60*, 7366-7375.

[72] D. Feng, F. Cao, L. Hou, T. Li, Y. Jiao and P. Wu, *Small* **2021**, *17*, e2103195.
[73] S. Liu, J. Mao, W. K. Pang, J. Vongsvivut, X. Zeng, L. Thomsen, Y. Wang, J. Liu, D. Li and Z. Guo, *Adv. Funct. Mater.* **2021**, *31*, 2104281.
[74] Y. Wu, Z. Zhu, D. Shen, L. Chen, T. Song, T. Kang, Z. Tong, Y. Tang, H. Wang and C. S. Lee, *Energy Storage Mater.* **2021**, 10.1016/j.ensm.2021.1011.1003.
[75] W. Yang, X. Du, J. Zhao, Z. Chen, J. Li, J. Xie, Y. Zhang, Z. Cui, Q. Kong, Z. Zhao, C. Wang, Q. Zhang and G. Cui, *Joule* **2020**, *4*, 1557-1574.
[76] D. Han, C. Cui, K. Zhang, Z. Wang, J. Gao, Y. Guo, Z. Zhang, S. Wu, L. Yin, Z. Weng, F. Kang and Q.-H. Yang, *Nat. Sustain.* **2021**, https://doi.org/10.1038/s41893-41021-00800-41899.
[77] J. Shi, T. Sun, J. Bao, S. Zheng, H. Du, L. Li, X. Yuan, T. Ma and Z. Tao, *Adv. Funct. Mater.* **2021**, *31*, 2102035.
[78] L. Cao, D. Li, F. A. Soto, V. Ponce, B. Zhang, L. Ma, T. Deng, J. M. Seminario, E. Hu, X. Q. Yang, P. B. Balbuena and C. Wang, *Angew Chem Int Ed Engl* **2021**, *60*, 18845-18851.
[79] T. Sun, S. Zheng, H. Du and Z. Tao, *Nano-micro Lett.* **2021**, *13*, 204.
[80] X. Lin, G. Zhou, M. J. Robson, J. Yu, S. C. T. Kwok and F. Ciucci, *Adv. Funct. Mater.* **2021**, 2109322.
[81] M. Zhu, X. Wang, H. Tang, J. Wang, Q. Hao, L. Liu, Y. Li, K. Zhang and O. G. Schmidt, *Adv. Funct. Mater.* **2019**, *30*.
[82] X. Lin, G. Zhou, J. Liu, M. J. Robson, J. Yu, Y. Wang, Z. Zhang, S. C. T. Kwok and F. Ciucci, *Adv. Funct. Mater.* **2021**, *31*.
[83] S. Cai, X. Chu, C. Liu, H. Lai, H. Chen, Y. Jiang, F. Guo, Z. Xu, C. Wang and C. Gao, *Adv. Mater.* **2021**, *33*, e2007470.
[84] H. Qiu, R. Hu, X. Du, Z. Chen, J. Zhao, G. Lu, M. Jiang, Q. Kong, Y. Yan, J. Du, X. Zhou and G. Cui, *Angew. Chem. Int. Ed.* **2021**.
[85] Y. Zhao, Y. Ding, Y. Li, L. Peng, H. R. Byon, J. B. Goodenough and G. Yu, *Chem. Soc. Rev.* **2015**, *44*, 7968-7996.
[86] C. Zhang, L. Zhang, Y. Ding, X. Guo and G. Yu, *ACS Energy Lett.* **2018**, *3*, 2875-2883.
[87] S. C. Wu, M. C. Tsa, H. J. Liao, T. Y. Su, S. Y. Tang, C. W. Chen, H. A. Lo, T. Y. Yang, K. Wang, Y. Ai, Y. Z. Chen, L. Lee, J. F. Lee, C. J. Lin, B. J. Hwang and Y. L. Chueh, *ACS Appl Mater Interfaces* **2022**, *14*, 7814-7825.
[88] Y. Yang, S. Liang, B. Lu and J. Zhou, *Energy & Environmental Science* **2022**, https://doi.org/10.1039/D1031EE03268B.
[89] C. Zhang, H. Chen, Y. Qian, G. Dai, Y. Zhao and G. Yu, *Adv. Mater.* **2021**, *33*, e2008560.
[90] Masakazu Matsumoto, Shinji Saito and I. Ohmine, *Nature* **2002**, *416*, 409–413.
[91] D. Han, C. Cui, K. Zhang, Z. Wang, J. Gao, Y. Guo, Z. Zhang, S. Wu, L. Yin, Z. Weng, F. Kang and Q.-H. Yang, *Nat. Sustain.* **2021**, 10.1038/s41893-41021-00800-41899.
[92] L. Cao, D. Li, F. A. Soto, V. Ponce, B. Zhang, L. Ma, T. Deng, J. M. Seminario, E. Hu, X. Q. Yang, P. B. Balbuena and C. Wang, *Angew. Chem. Int. Ed.* **2021**, *60*, 18845-18851.
[93] H. Du, K. Wang, T. Sun, J. Shi, X. Zhou, W. Cai and Z. Tao, *Chem. Eng. J.* **2022**, *427*, 131705.
[94] J. Hao, L. Yuan, C. Ye, D. Chao, K. Davey, Z. Guo and S. Z. Qiao, *Angew. Chem. Int. Ed.* **2021**, *60*, 7366-7375.
[95] Y. Yamada, K. Usui, K. Sodeyama, S. Ko, Y. Tateyama and A. Yamada, *Nat. Energy* **2016**, *1*, 16129.
[96] Y. Lv, Y. Xiao, L. Ma, C. Zhi and S. Chen, *Adv. Mater.* **2021**, e2106409.
[97] Q. Nian, J. Wang, S. Liu, T. Sun, S. Zheng, Y. Zhang, Z. Tao and J. Chen, *Angew. Chem. Int. Ed.* **2019**, *58*, 16994-16999.
[98] Y. Ye, Y. Zhang, Y. Chen, X. Han and F. Jiang, *Adv. Funct. Mater.* **2020**, *30*.

[99] X. Zeng, J. Mao, J. Hao, J. Liu, S. Liu, Z. Wang, Y. Wang, S. Zhang, T. Zheng, J. Liu, P. Rao and Z. Guo, *Adv. Mater.* **2021**, *33*, e2007416.
[100] M. Yan, N. Dong, X. Zhao, Y. Sun and H. Pan, *ACS Energy Lett.* **2021**, *6*, 3236-3243.
[101] Y. Gao, Z. Liu, S. Guo, X. Cao, G. Fang, J. Zhou and S. Liang, *Energy Environ. Mater.* **2021**.
[102] X. Dong, Z. Guo, Z. Guo, Y. Wang and Y. Xia, *Joule* **2018**, *2*, 902-913.
[103] H. Zhang, J. M. Vicent-Luna, S. Tao, S. Calero, R. J. Jiménez Riobóo, M. L. Ferrer, F. del Monte and M. C. Gutiérrez, *ACS Sustainable Chem. Eng.* **2022**, 10.1021/acssuschemeng.1021c06999.
[104] A. Wulf, K. Fumino and R. Ludwig, *Angew. Chem. Int. Ed.* **2010**, *49*, 449-453.
[105] a) Y. Zhu, X. Guo, Y. Lei, W. Wang, A.-H. Emwas, Y. Yuan, Y. He and H. N. Alshareef, *Energy & Environmental Science* **2022**, https://doi.org/10.1039/D1031EE03691B; b) S. Kumar, T. Salim, V. Verma, W. Manalastas and M. Srinivasan, *Chemical Engineering Journal* **2022**, *435*; c) Y. Bian, W. Jiang, Y. Zhang, L. Zhao, X. Wang, Z. Lv, S. Zhou, Y. Han, H. Chen and M. C. Lin, *ChemSusChem* **2022**, *15*, e202101398; d) J. Hwang, A. N. Sivasengaran, H. Yang, H. Yamamoto, T. Takeuchi, K. Matsumoto and R. Hagiwara, *ACS Appl Mater Interfaces* **2021**, *13*, 2538-2546.

Dr. Xuejun Lu received his Ph.D. at Instituto de Ciencia de Materiales de Madrid (ICMM, Spain) under the supervision of Prof. Francisco del Monte and Dr. María Concepción Gutiérrez in July 2021. He is currently a postdoc research fellow in Prof. Jian Liu's group at the University of British Columbia (UBC, Canada). His research now focuses on advanced aqueous electrolytes via designing eutectic liquid mixtures for the implementation of electrochemical energy storage devices.

Evan Hansen received his B.ASc. from The University of British Columbia (UBC, Canada) in 2020. He is currently working towards his Ph.D under the supervision of Dr. Jian Liu at The University of British Columbia (UBC, Canada) within Dr. Liu's Advanced Materials for Energy Storage group. His research focus is towards the development of improved zinc-ion batteries using aqueous and solid-state electrolytes, separator development, and anode interphase designs.

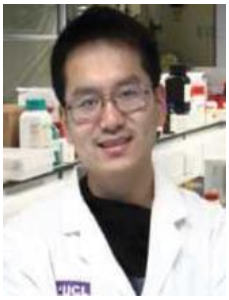

Dr. Guanjie He is an associate professor in materials chemistry at the University of Lincoln and an honorary lecturer at University College London (UCL). Dr. He received Ph.D. Degree in Chemistry, UCL under the supervision of Prof. Ivan P. Parkin. Dr. He's research focuses on materials design for electrochemical energy storage and conversion applications.

Dr. Jian Liu is an Assistant Professor and Principal's Research Chair in Energy Storage Technologies at the University of British Columbia (UBC) Okanagan campus, Canada. Dr. Liu received his Ph.D. in materials science (2013) from the University of Western Ontario (Canada) and worked as an NSERC Postdoctoral Fellow at Lawrence Berkeley National Laboratory and Pacific Northwest National Laboratory before joining UBC in January 2017. His current research interests focus on advanced nanofabrication techniques, materials design for Li-ion batteries and beyond, and interfacial control and understanding in energy storage systems.

The table of contents

Eutectic Electrolytes Chemistry for Rechargeable Zn Batteries

Xuejun Lu [a], Evan J Hansen [a], Guanjie He [b,c], Jian Liu [a]*

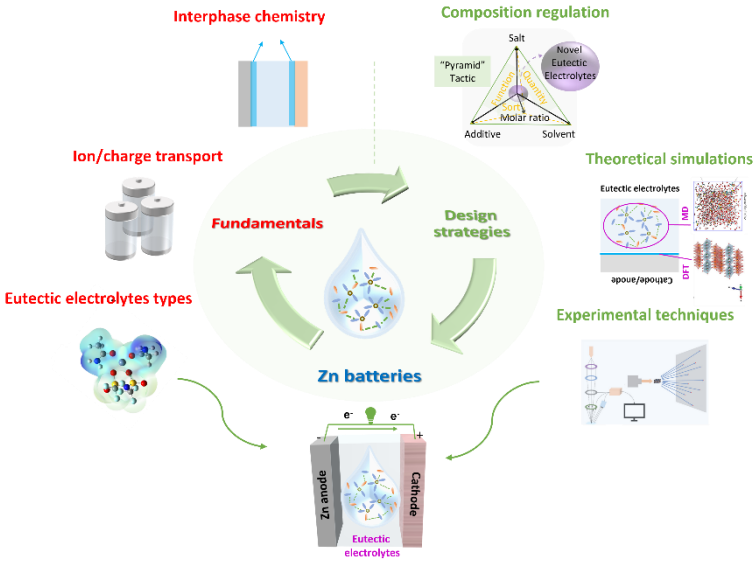

Eutectic electrolytes are promising alternatives for high-performance rechargeable Zn batteries (RZBs). This review presents fundamentals and design strategies of eutectic electrolytes for the development of Zn battery implementations. Moreover, the comprehensive summary of eutectic electrolytes in practical RZB utilization offers enormous opportunities and open appealing prospects.